4

Propagation Prediction Models

Dieter J. Cichon [1], IBP PIETZSCH GmbH, Germany
Thomas Kürner [1], E-Plus Mobilfunk GmbH, Germany

4.1 General Considerations

To implement a mobile radio system, wave propagation models are necessary to determine propagation characteristics for any arbitrary installation. The predictions are required for a proper coverage planning, the determination of multipath effects as well as for interference and cell calculations, which are the basis for the high-level network planning process. In a GSM/DCS-system the high-level network planning process includes, e.g., frequency assignment and the determination of the BSS (base station subsystem) parameter set. Similar planning tasks will exist also in third generation systems. The environments where these systems are intended to be installed, are stretching from in-house areas up to large rural areas. Hence wave propagation prediction methods are required covering the whole range of macro-, micro- and pico-cells including indoor scenarios and situations in special environments like tunnels and along railways. The phenomena which influence radio wave propagation can generally be described by four basic mechanisms: Reflection, penetration, diffraction, and scattering. For the practical prediction of propagation in a real environment these mechanisms must be described by approximations. This requires a three-stage modelling process: In the first step the real (analogue) terrain has to be digitised yielding digital terrain data. Therefore some interest in the COST 231 project has focused on the types, resolution and accuracy of digital terrain databases required for propagation modelling. The information includes terrain height information, land usage data, building shape and height information and building surface characteristics. Furthermore investigations have

---

[1] Formerly with University of Karlsruhe, IHE, Germany

been stressed on proper processing techniques to extract the relevant information in a time-efficient manner. These topics are described in Sec. 4.2. The second modelling step includes the definition of mathematical approximations for the physical propagation mechanisms. Therefore Sec. 4.3 treats basic problems as e. g. the diffraction around a non-perfectly conducting wedge, simulating a street corner and the modelling of propagation over roof-tops. Based on the solutions for the basic problems both deterministic and empirical approaches have been developed within COST 231 for the various environments, which is the third modelling step. In the different environments distinctions of the models are required both in terms of the dominant physical phenomena and the specification of the digital terrain data. In Sec. 4.4, 4.5, 4.7 and 4.8 all models dedicated for the same environment and cell type are treated in separate sections. Sec. 4.6 deals with building penetration models, which are applicable to all cell types. As the definition of cell types is not unique in the literature, the cell type definition used in this chapter is explained more detailed.

cell type	typical cell radius	typical position of base station antenna
macro-cell (large cell)	1km to 30 km	outdoor; mounted above medium roof-top level, heights of all surrounding buildings are below base station antenna height
small macro-cell	0.5 km to 3 km	outdoor; mounted above medium roof-top level, heights of some surrounding buildings are above base station antenna height
micro-cell	up to 1 km	outdoor; mounted below medium roof top level
pico-cell / in-house	up to 500 m	indoor or outdoor (mounted below roof-top level)

Tab. 4.1.1 Definition of cell types.

In "large cells" and small cells" the base station antenna is installed above roof-tops. In this case the path loss is determined mainly by diffraction and scattering at roof-tops in the vicinity of the mobile, i. e. the main rays propagate above the roof tops. In "micro-cells" the base station antennas are mounted generally below roof tops. Wave propagation is determined by diffraction and scattering around buildings, i. e., the main rays propagate in street canyons somehow like in grooved waveguides. "Pico-cells" are applied to cover mainly indoor or very small outdoor areas. In any case the base station antenna of a pico-cell is mounted inside a building or fairly below roof-top level in outdoors. The summary of the different cell types is shown in Tab. 4.1.1.

4.2 Geographical Information for Propagation Modelling and Simulation

Peter J. Cullen , University of Dublin, Trinity College, Ireland

The practice of the determination of radio channel characteristics in cellular UHF land mobile radio applications is dominated by surface scattering considerations. Before any propagation (scattering) computation can be performed, these surfaces must be characterised. In this brief section an outline is given of some of the basic issues relating to the use of geographical information in mobile radio communications from a propagation perspective, drawing exclusively from the experience of COST 231.

The development of propagation prediction techniques for the estimation of channel characteristics is a cyclic, three stage process: the first step is to abstract the simplest surface model which is considered to be likely to yield sufficiently accurate predictions; the second stage is concerned with finding efficient (often approximate or numerical) solutions to the scattering problems thus posed; and the third stage is to verify the choice made in the first stage. In each of these stages one must make use of geographical information.

4.2.1 Canonical scattering problems

Before embarking on the review, it is essential to consider the problem to be solved. Ostensibly, the characterisation of the land mobile radio channel in a particular locality is of interest. To achieve this one must tackle the physical problem of the prediction of the scattering of UHF electromagnetic radiation. It is possible to express this problem formally but aside from the obvious computational difficulties involved, it is not possible even in principle, to find exact complete solutions, since the actual scatterer can never be really specified to a sufficiently high degree of accuracy (this is not the case in any general sense for the canonical surfaces described below). Scattering is a non-linear problem, small deviations in the surface do not necessarily lead to small deviations in the fields everywhere, especially the near fields. Fortunately, one is usually not particularly interested in the very near field and, as a consequence, the modelling exercise is carried out as described in the introduction. In the main, the canonical problems that are employed are relatively simple.

One-dimensional surfaces.

The most familiar canonical problem in land mobile propagation is the corrugated one-dimensional perfect electrical conducting (PEC) surface. In this case, if the propagation is TMz or TEz the electromagnetic problem is a scalar one. Moreover, if the surface is smooth and the angle of incidence low, forward propagation will predominate. This model may be enhanced by considering the surface to be a homogeneous dielectric, further enhancements can be achieved by considering a piece-wise homogeneous dielectric. This kind of canonical model has found very wide acceptance for predicting attenuation of low angle wave propagation over irregular terrain. The primary geometrical entity to be acquired here is the surface height profile. Finite difference [1] and integral equation [2] schemes operate directly on the surface height profile. When a parabolic equation approximation is applied to the Helmholtz equation calculations can be performed using the split step method [3]. When larger steps are used this leads to a method often (inaccurately) associated with absorbing screens. Native ray-tracing approaches represent the surface by an ensemble of canonical shapes (wedges and cylinders) for which diffraction or reflection coefficients exist, in practice this approach must be rather arbitrary. Typically, the corrugated two-dimensional canonical problem is used for propagation modelling over irregular terrain. It may also arise in urban and micro-cell problems, when a two-dimensional (vertical plane) approach is followed. Over terrain, predictions are usually corrected locally through the use of clutter information which is derived from remotely sensed optical data. The height profile (array of heights) associated with this canonical problem is usually derived from the databases during the computation of the fields.

Unconnected one-dimensional surfaces arise when we consider propagation in the horizontal plane. When calculating fields around buildings, where the antenna heights are well below roof-top height and the terrain is flat (simple micro-cell case), it can be sufficient to use multiple paraxial PEC cylinders (by cylinder we mean a two-dimensional entity) to represent the buildings; where the cross-section of the cylinders is the building plan outline. This is the case for example for the most simple two-dimensional micro-cell models. Further enhancements include the use of homogeneous or piece-wise homogeneous (to allow the representation of internal and external structure) dielectric cylinders. The most natural (and increasingly popular) data structure for this type of problem is the vector (polygon) database. Each discrete cylinder is represented by one or more polygons. If appropriate, attributes (percentage of windows for example) may be attached to the faces

of the polygons to facilitate the refinement of propagation models. The vector storage data structure is well suited to ray-tracing, ray-launching and hybrid methods. The polygon structure is also capable of efficiently delivering the geometrical input requirements of other methods for handling this kind of problem including integral equation techniques, transmission line method (TLM), finite difference time domain (FDTD) etc.

Two-dimensional surfaces.

An increasingly important canonical problem of interest is the two-dimensional smooth surface. This surface, like its one-dimensional counterpart, may be assumed to be homogeneous PEC, dielectric or piece-wise homogeneous dielectric. Considering the level of accuracy required in mobile propagation the most appropriate representation here is a triangular regular network (the analogue of piece-wise linear representation used in the one-dimensional case). Increased resolution may be obtained by using a triangular irregular network (TIN), or a multi-scale regular network. An outward normal is generally stored for each facet; other attributes such as roughness measures and land use classifications may be attached directly to the facets.

The most complex two-dimensional surfaces (three-dimensional databases) arise when we have to consider propagation in and around buildings located on irregular terrain. The main differences between this case and the previous one is the abrupt changes in surface height which occur at the location of building walls and in the possibility of inhomogeneity (rooms, windows etc. in buildings). This kind of data may be handled using a TIN structure if homogeneous, or more appropriately, using a vector structure. It is quite popular to consider a hybridisation of regular elevation matrix, (for the terrain) and polygon (for buildings). A fairly typical approach is described in [4], [5].

Networks are not used to characterise scattering surfaces but are important for certain propagation related tasks. Typically networks are used to efficiently locate roads, streets, railway lines etc. Some micro-cell propagation models can predict using this kind of information as a starting point. More importantly, the road networks are important areas in which to guarantee coverage.

4.2.2 Acquisition of geographical data

There is little point in constructing accurate propagation methods if the geographical data which these methods rely upon is not correspondingly accurate. Traditionally, this kind of information has been obtained from paper maps. In the last decade increasing use has been made of high resolution remote sensing (aerial and satellite) for acquisition and of digital storage and distribution methods. The generation of Digital Elevation Models (DEM) and the efficient and accurate extraction of radial data from them is reviewed in [6].

Satellite remotely sensed data may be obtained from optical sources: LandSat (30m resolution), SPOT (10-20m resolution) and synthetic aperture radar (SAR) sources: ERS-1. SPOT and LandSat have been used to derive land use classes for terrain. The methodology of extraction is beyond the scope of this book. The use of SAR in propagation prediction is an open research question.

Micro-cell and indoor propagation modelling possess the heaviest reliance on high resolution geographical information. High resolution (1-2m) databases derived from aerial photography measurements are now being used by a number of organisations, particularly for cities (see also Sec. 4.5). For urban propagation, it is essential to have accurate information at least about the average height of individual buildings, when modelling larger cells or performing interference calculations and when terminals are operating close to roof-top height. It may not be so important in the case of line-of-sight links. The incorporation of information about clutter, particularly vegetation, is very important, since propagation characteristics are quite sensitive to scatterers around terminals.

Aerial stereo photography provides a means of obtaining quite accurate data on the heights and outlines (resolution of the order 1m) of building and terrain features, the location of vegetation etc. A wealth of data can, in principle, be extracted from these sources. However, the extraction of data is quite labour intensive. Sometimes such data is combined with lower resolution regular elevation matrices, in principle (but not always in practice) this should not be necessary (ground height can be accurately determined from aerial photography) this should really be avoided where possible in micro-cell work.

Information about the building cladding, windows, etc. is more difficult to obtain. It appears that accurate geographical information of this nature must

be obtained „on the ground“ as it were (using video cameras to capture data, for example). To date there appear to be few, if any, physical propagation models capable of using this kind of information (there are empirical methods). Wall properties are particularly important for estimating building penetration. For outdoor propagation, in practice we may only need this level of detail around potential BTS sites.

Considering indoor propagation [7] suggests, for the purpose of propagation modelling, that each building element should be categorised into {wall, floor, door, window, furniture,...} and specified by structure (thickness and permittivity) and finally its corner co-ordinates (twelve co-ordinates).

4.2.3 Accuracy of data

Recalling that field estimates *may* be quite sensitive to surface errors, the following observations are recorded. Considering the database for the city of Munich (see Sec. 4.5), it is shown in [8] that the average difference in predictions for over-roof-top propagation estimates using a mean roof-top height and the real roof-top heights is about 4dB. The average was over an area of 2400-3400 m, the database used had a 5 m resolution and the standard deviation of the building heights was 8.56 m and that of the terrain height was 3.87 m. Considering the influence of database information on prediction accuracy it is noted in [9] that prediction errors in micro-cells of up to 15 dB were attributed to database inaccuracies arising from the omission of vegetation data and the poor resolution of terrain height data. Perturbing the scatterers (specifically: wall vector directions) in a micro-cell type problem using a two-dimensional Geometrical Theory of Diffraction (GTD) approach is shown to have a significant effect on the structure of field predictions [10]. These results are indicative of what is expected, average field estimates or field estimates very far away from a multi-scale scatterer are likely to be less sensitive to the smaller scale errors. Whereas the location of an interference null or shadow boundary may manifest a much higher sensitivity.

One rather practical point to be aware of, is that geographical information (aside from resolution limitations) is prone to contain errors. It is always advisable to visually inspect data and carry out any corrections prior to use.

4.2.4 Model evaluation

In the previous section some brief consideration to the effect of database errors in field estimates is given. Probably one of the most important causes

of concern here is the effect of database inaccuracies on model evaluation. Complex models which visually correspond to the measured data often display a large error standard-deviation with respect to empirical models because of spatial offsets (see Sec. 4.5). These offsets can arise if there are small database or measurement location errors. The existence of these offsets between predictions and measurements is not necessarily an indication of a poor model. This problem is typically addressed by separately comparing the locally averaged model prediction and the statistics of the faster variations separately with the measured data.

As the micro-cell work develops and different competing solutions emerge a rigorous and standard approach is needed to compare the different models on the same data. This requires agreed simple procedures for comparing model predictions with measurements and with each other. For example, in relation to the question of the determination of the number of rays required for a ray-optical approach it is useful to consider ways of implementing the null hypothesis test that the addition of an extra ray-path does not explain any more of the data. This must be done in the light of uncertainties in the measurement location and geographical data; this would suggest a more formal probabilistic approach to model evaluation.

4.2.5 Manipulation of geographical data

The reader should be aware that there is a wide range of commercial geographic information systems (GIS) which may be employed to manipulate and process geographical data; for example ARC-INFO [6], and SMALLWORLD [11]. COST 231 has not made a special study of these types of systems and it is beyond the scope of this book to make any comments as to the applicability or suitability of such commercial systems to propagation prediction. Aside from direct application in propagation modelling GIS functionality is clearly essential in preparing data for the construction of a propagation specialised database.

However, it is clear that the organisation and representation of geographical information is crucial to the provision of computationally efficient propagation estimates. Many methods used in mobile radio propagation rely on high frequency approximations and require detailed geometrical computations to be made on a basic data-set describing the environment. One such example is GTD which requires the identification of geometric ray paths. Once one has chosen to use basic GTD, methods for mobile propagation, the computational problem becomes primarily a geometric one. It is pointed out in [12] that hierarchical geometrical structures [13] can be

applied to buildings databases to aid in reducing the complexity of ray-optical approaches. To clarify the point we include the example they gave to illustrate the approach: consider a complex multifaceted building - intersections of a given ray will have to be considered for each of the facets. However, if we encapsulate the building in a simple rectangular polygon oriented parallel to the co-ordinate axes then it is a simple task to determine whether or not a ray enters this box; only if it does, we need to calculate intersections with the building facets. They add that this principle can obviously be applied not only to single buildings but also to clusters of buildings and so on. Another point is that, whilst high resolution building data is becoming increasingly widely available; from a practical point of view, one may wish to remove some of the detail (small recesses, for example) prior to using ray-optical methods, in order to keep complexity to manageable levels. Finer detail is important when one is interested in the near field and this might suggest a combination of full resolution and smoothed database for ray applications.

4.2.6 Exchange of measurement and geographic information

Radio measurement data formats have been the subject of some discussion in COST 231. Two suggestions which have been formally specified are the RACE [14]format and the universal measurement format (UMF) [15]. It appears that the DXF and regular matrix formats are adequate for the exchange of typical geographical information used by the land mobile radio propagation community.

4.3 Propagation Mechanisms

Jean-Frédéric Wagen , Swisscom, Switzerland

4.3.1 General

This section describes the radio propagation mechanisms that have been investigated within the COST 231. The propagation mechanisms are examined to help the development of propagation prediction models and to enhance the understanding of electromagnetic wave propagation phenomena involved when dealing with radio transmission in mobile and personal communications environments.

Evidently the radio propagation phenomena are by themselves not new and do not depend on the environment considered. However, considering all existing radio propagation phenomena, the most important one must be identified and investigated to improve the modelling of the mobile radio communication channel or of the prediction of radio coverage and signal quality in radio communication systems. The radio propagation phenomena to be identified as the most important depend on the environment and differ whether we consider flat terrain covered with grass, or brick houses in a suburban area, or buildings in a modern city centre etc. Propagation models are more efficient when only the most dominant phenomena are taken into account. Which radio propagation phenomena need to be taken into account and in how much detail do they need to be considered will also differ whether we are interested in modelling the average signal strength, or a fading statistic, or the delay spread, or any other characteristics.

The mobile radio environment causes some special difficulties to the investigation of propagation phenomena:

1) The distances between a base station and a mobile range from some metres to several kilometres,
2) man-made structures and natural features have size ranging from smaller to much larger than a wavelength and affect the propagation of radio waves,
3) the description of the environment is usually not at our disposal in very much detail.

Roughly two complementary approaches can be identified to deal with these difficulties:

- *Experimental investigations* which are closer to the reality but at the expense of weaker control on the environment, and
- *theoretical investigations* which consider only simplified model of the reality but give an excellent control of the environment.

A brief description of the possibilities, advantages and disadvantages offered by either experimental or theoretical investigations are given below to give some insights on how the propagation phenomena can be determined.

Experimental investigations.

Based on measurements, the propagation mechanisms can be identified if the experiments are thoughtfully designed in a carefully chosen area or/and if numerous measurements are analysed. Several contributions to COST 231 have investigated the propagation phenomena from measurements (e.g., [16]-[18]).

Note that scaled measurements ease the control on the environment to be investigated. However, scaled measurements are scarce since they require special hardware and could be quite difficult to conduct in a worthwhile manner because of the difficulties of retaining just the right amount of complexity in the simplified scaled down model. Only a single contribution dealing with measurements in scaled tunnels has been presented to COST 231 (Section 4.8.5).

The major disadvantage of experimental investigations is the difficulties in the design of the experiments and in the interpretation of the results which usually exhibit a mix of several propagation phenomena.

Theoretical investigations.

Software simulation or analytical studies of propagation phenomena have one main advantage over experimental investigations: The environment and the geometry are more easily described and modified. The major disadvantage of theoretical investigations is that the validity of the results may hold only for the particular case being simulated or investigated. Theoretical investigations should always be validated in practice. The theoretical investigations can be categorised in two approaches (see Fig. 4.3.1 and Fig. 4.3.2):

1) Simulation of wave propagation, and

2) ray theory.

Simulation of wave propagation.

Considering Maxwell´s equations or the wave-equation and some boundary conditions, the electromagnetic wave propagation mechanisms can be investigated from a pure theoretical point of view and from computations based on so-called full-wave formulations. This approach is conceptually similar to performing actual measurements but the "simulated measurements" have the advantage of providing a much better control over the propagation environments. As with measurements however, extracting the various physical phenomena and their relative contributions from the simulation results requires further analysis.

Ray theory.

Some simplifications in solving the wave propagation problems are obtained when assuming a small wavelength which leads to view the radio wave propagation as rays similar to light rays. Under this assumption, the radio wave interacts with the propagation environment, i.e., with the atmosphere, the terrain features, buildings, walls, trees, etc., through absorption, specular reflection, diffraction and scattering. At a larger scale, several rays can be viewed as a single entity and according to this concept, guided propagation has been investigated.

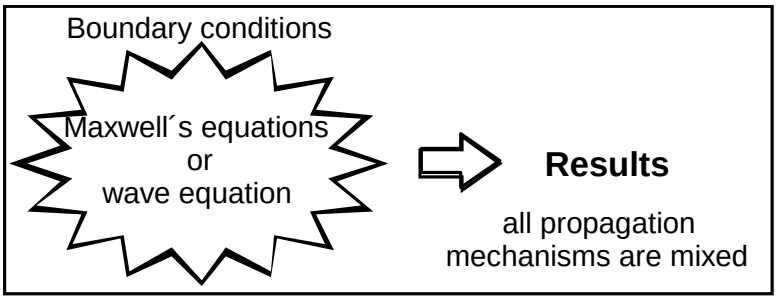

Fig. 4.3.1 Simulation of wave propagation.

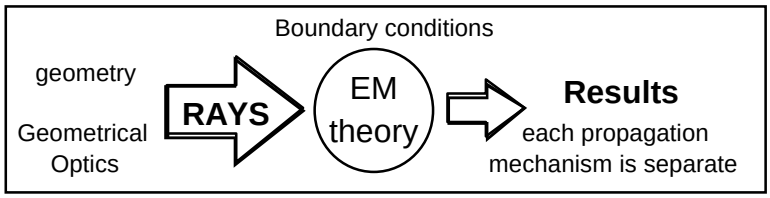

Fig. 4.3.2 Ray theory.

The ray theory approach clearly distinguishes between several propagation phenomena and give to each of them a physical and mathematical description. How clearly the ray theory propagation phenomena exist in practice depends on the frequency, on the environments and on how precisely the prediction and measurement results are analysed.

The next section reviews the propagation mechanisms relevant to the ray theory. To complement the discussion, other propagation mechanisms are mentioned in Sec. 4.3.3. The last Sect. 4.3.4 mentions the propagation mechanisms which appear to be the most important for propagation modelling and prediction in macro-cellular, micro-cellular and indoor environments.

4.3.2 Propagation mechanisms in the ray theory

The main propagation mechanisms defined by the ray theory are explained below. As smaller wavelengths, i.e., higher frequencies are considered, the wave propagation becomes similar to the propagation of light rays. A radio ray is assumed to propagate along a straight line bent only by refraction, reflection, diffraction or scattering. These are the concepts of Geometrical Optics. There is no transversal dimension associated to the rays. However, the finite size of the wavelength at radio frequencies leads to hinder in some ways the assumption of infinitely thin rays. Related to the "thickness" of a radio ray is the concept of Fresnel zones. A Fresnel zone is the locus of points (R) around the source (S) and an observation point (Ob) such that the phase on the path S-R-Ob equals the sum of the phase on the shortest distance S-Ob plus an additional constant (Fig. 4.3.3). When this phase difference equals p, the direct ray (S-Ob) and the reflected or scattered ray (S-R-Ob) are out of phase and the locations of points defines the so-called first Fresnel zone.

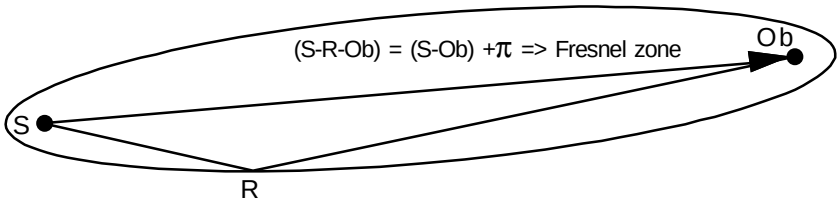

Fig. 4.3.3 The first Fresnel zone.

Specular reflection

The specular reflection phenomena is the mechanism by which a ray is reflected at an angle equal to the incidence angle. The reflected wave fields are related to the incident wave fields through a reflection coefficient which is a matrix when the full polarimetric description of the wave field is taken into account. The most common expression for the reflection is the Fresnel reflection coefficient which is valid for an infinite boundary between two mediums, for example: air and concrete. The Fresnel reflection coefficient depends upon the polarisation and the wavelength of the incident wave field and upon the permittivity and conductivity of each medium. The application of the Fresnel reflection coefficient formulas is very popular in ray tracing software tools.

Some authors (e.g. [19]-[21]) consider constant reflection coefficients to simplify the computations. However the validity of a constant reflection coefficient is usually not investigated. Considering building penetration (Sec. 4.6.2) or indoor propagation [22], some authors showed an improved fit to measurements by using reflection and transmission coefficients varying with the incidence angle instead of constant coefficients (Sec. 4.7.2).

Specular reflections are mainly used to model reflection from the ground surface and from building walls (see Sec. 4.5 and Sec. 4.7.5). The mechanisms of specular reflections have been used to interpret measurements in some particular environments such as high rise city centre [23], micro-cells [16], indoor [17] and down in a street canyon illuminated from over the roof ("Reflections from buildings next to the mobile" [24], [25]). Whether scattering (1/(d1• d2) dependence) or truly specular reflection (1/(d1+d2) dependence) is the proper propagation phenomena was not mentioned and cannot be readily determined since the two phenomena are usually involved simultaneously.

It is pointed out that reflection from a finite surface is not considered in this section since it can be seen either as the sum of the two phenomena specular reflection and edge diffraction, or as a scattering process.

Diffraction

The diffraction process in ray theory is the propagation phenomena which explain the transition from the lit region to the shadow regions behind the corner of a building or over the roof-tops. Diffraction by a single wedge can be solved in various ways: empirical formulas [26], [27]. Perfectly Absorbing Wedge (PAW) [28], [29], Geometrical Theory of Diffraction

(GTD) [29], [30], Uniform Theory of Diffraction (UTD) [31] or even more exact formulations [32], [33]. The advantages and disadvantages of using either one formulation is difficult to address since it may not be independent on the environments under investigations. Indeed, reasonable results are claimed for each formulations. The various expressions differs mainly from the approximations being made on the surface boundaries of the wedge considered. One major difficulty is to express and use the proper boundaries in the derivation of the diffraction formulas. Another problem is the existence of wedges in real environments: the complexity of a real building corner or of the building roofs clearly illustrates the modelling difficulties. Despite these difficulties, however, diffraction around a corner or over a roof-top are commonly modelled using the heuristic UTD formulas [34] since they are fairly easy to program, are well behaved in the lit/shadow transition region, and account for the polarisation and the wedge material.

Multiple diffraction

For the case of multiple diffraction, the complexity increases dramatically. In the case of propagation over roof-top the results of Walfisch and Bertoni [24] has been used to produce the COST-Walfisch-Ikegami model (Sec. 4.4.1). The approximate procedures of Giovannelli [35] or Deygout [25], [36] have been revisited by some authors. The limitations of these approximations lead several researchers to more accurate methods: SIP/FFT [37], [38] (Sec. 4.4.3, PEM), Integral Equation (Sec. 4.4.3, MFIE), Heat Wave Parabolic Equation (Sec. 4.4.3, PEM), Reduced Integral Operator (Sec. 4.4.3, EFIE), Flat Edge Model [39], Slope Diffraction [40]. All these methods are numerical schemes to compute the multiple diffraction and apart from the last contribution they do not give a clear physical understanding of the multiple diffraction process, at least not yet.

One method frequently applied to multiple diffraction problems is UTD. The main problem with straightforward applications of the UTD is, that in many cases one edge is in the transition zones of the previous edges. Strictly speaking this forbids the application of ray techniques, but in the spirit of UTD the principle of local illumination of an edge should be valid. At least within some approximate degrees, a solution can be obtained. In [41] a solution is shown that is quite accurate in most cases of practical interest. The key point in the theory is to include slope diffraction, which is usually neglected as a higher order term in an asymptotic expansion, but in transition zone diffraction the term is of the same order as the ordinary amplitude diffraction terms [40]. Another key element in the method is automatic enforcement of continuity of amplitude and slope at each point.

For the case of diffraction over multiple screens of arbitrary heights and spacings a solution is obtained within the frame of UTD. This solution agrees to a good approximation within the known results for constant spacing and with numerical results using Vogler's solution [42]. The limitation of the method is, that it is not applicable when one spacing becomes very small relative to other spacings. Thus the method cannot predict the collapse of two screens into one.

In ITU-R 526-2 [43] equations are given to compute effects of multiple diffractions around curved cylinders. In [44], an investigation of this method revealed that a modification of the ITU equations yields good results even for multiple knife-edge diffraction. The diffraction losses for the single obstacles are replaced by the diffraction losses for single knife edges. Furthermore, the following modified correction factor C_N has to be used:

$$C_N = \frac{P_a}{P_b} \tag{4.3.1}$$

The ITU equations are simple to apply and can account for knife-edges with unequal heights and separations. In the special case of grazing incidence over a series of equal distance and equal height knife-edges, the modified ITU equations yield the correct analytical results [40]. This holds true even for very large numbers of edges. The modified ITU method is also compared to the Maciel-Bertoni-Xia-method [45]. Results with the same slope versus the number of edges are achieved. However compared to [45] the path loss is lower (higher), when the transmitter is below (above) the knife-edges.

Scattering

Rough surfaces and finite surfaces scatter the incident energy in all directions with a radiation diagram which depends on the roughness and size of the surface or volume. The dispersion of energy through scattering means a decrease of the energy reflected in the specular direction. This simple view leads to account for the scattering process only by decreasing the reflection coefficient and thus, only by multiplying the reflection coefficient with a factor smaller than one which depends exponentially on the standard deviation of the surface roughness according to the Raleigh theory [46]. This description do not take into account the true dispersion of radio energy in various directions, but accounts for the reduction of energy in the specular direction due to the diffuse components scattered in all other directions.

More realistic scattering processes have been investigated within the COST 231. Most investigations (Sec. 4.4.4) deals with the application of the bistatic radar equation to account for the scattering from hills or mountain slopes. A preliminary study investigated the scattering pattern from large irregularities on a building wall [47]. The concept promoted in that study was to model the scattering by equivalent sources of scattering located at the building corners. Further investigations are required to confirm and refine this concept.

Related to both rough surface scattering and diffraction, the theoretical models mentioned above using SIP/FFT, Integral Equation, Reduced Integral Operator, etc., to account for terrain scattering indicates that the forward scattering approaches lead to reasonable results (Sec. 4.4 and Sec. 4.5.3). This indicates that the back scattering in the radial plane from a given BS antenna is usually neglected or is not taken into account in a detailed manner. The influence of individual "urban" scatterers such as lamp post, traffic light, windows, and cars has not yet been investigated within the COST 231.

Penetration and absorption

Penetration loss due to building walls have been investigated and found very dependent on the particular situation (Sec. 4.6). Absorption due to trees (Sec. 4.4.2) or the body absorption (Sec. 3.4) are also propagation mechanisms difficult to quantify with precision.

Another absorption mechanism is the one due to atmospheric effects. These effects are usually neglected in propagation models for mobile communication applications at radio frequencies but are important when higher frequencies (e.g., 60 GHz) are used as described in Sec. 8.2.

4.3.3 Other propagation mechanisms

Guided wave

Wave guiding can be viewed as a particular propagation mechanism to describe the propagation in street canyon (Sec. 4.5.2 - Telekom model), in corridors or tunnels (Sec. 4.8). The wave guiding phenomena can be explained based on multiple reflections or propagation modes.

Atmospheric effects

Atmospheric effects are usually not taken into account for mobile radio applications at UHF frequencies, although empirical correction factors can

be incorporated in some coverage prediction tools to handle seasonal variations (Sec. 4.4.2).

4.3.4 Main propagation mechanisms

The main propagation mechanisms usually taken into account when modelling the radio propagation in macro-cell, micro-cell and indoor environments are visualised in Fig. 4.3.4. For different propagation mechanisms the range dependence of the field strength is given in the following:

- For *specular reflection* the field is proportional to $(d_1+d_2)^{-1}$,
- for *single diffraction*, the field is proportional to $(d_1/d_2(d_1+d_2))^{-0.5}$,
- for *multiple diffraction* and for a source illuminating all edges, the field is proportional to $d^{-1.9}$ [24],
- for *volume scattering* and *rough surface scattering*, the field is proportional to $(d_1 d_2)^{-1}$,
- for *penetration and absorption*, the field is mainly attenuated by a constant,
- for the *wave guiding* phenomena, the logarithm of the field is proportional to d.

In macro-cells

Forward propagation including multiple diffraction over terrain and buildings is used in most propagation prediction models for macro-cells (Sec. 4.4.1). Scattering or reflection from large buildings, hills, mountains are modelled to improve the prediction quality and especially to characterise the time dispersion of the radio channel (Sec. 4.4.3).

In micro-cells.

Most models rely only on specular reflection and diffraction phenomena. Some empirical formulations use guided wave (Sec. 4.5.2 - Telekom model and Uni-Karlsruhe 2D-URBAN-PICO model) or virtual source at intersections which can be viewed as a way to model the combined effects of diffraction and scattering (Sec. 4.5.2 - Ericsson model). Scattering effects from walls and trees as well as from individual scatterer such as balcony, lamp post, windows, cars, etc. remains to be carefully examined. Contributions from over-roof-top propagation are usually modelled using models similar to the ones for macro-cells (Sec. 4.5.3/ 4.5.4).

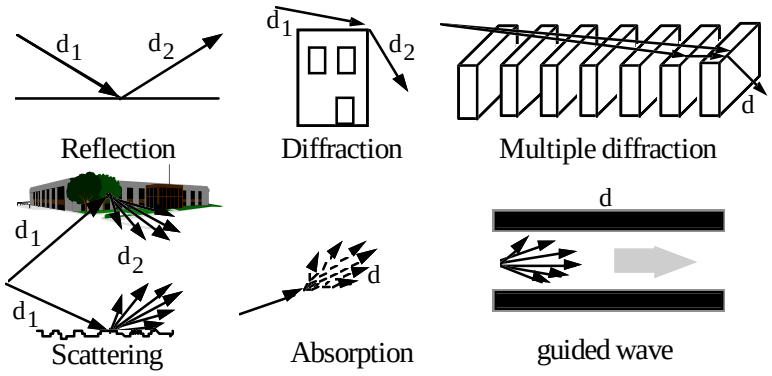

Fig. 4.3.4 **Propagation phenomena.**

Indoor

Mainly reflection from and transmission through walls, partitions, windows, floors, and ceilings are used to predict propagation within buildings (Sec. 4.6 and Sec. 4.7). Wave guiding in corridor or in hallways are more difficult to model and thus are usually not considered. Although diffraction effects have been sometime identified (Sec. 4.7.5), diffraction at edges from walls or windows is usually not taken into account due to the difficulties related to the requirement on the input database and due to the resulting large computation time.

4.4 Propagation Models for Macro-Cells

Thomas Kürner , E-Plus Mobilfunk GmbH, Germany

A considerable interest has been generated in finding solutions to predict average field strengths and multipath signals in macro-cells. The predictions are based on the knowledge of topography, land usage and building height information. This section deals with five different topics - modelling in urban areas, influence of vegetation, large-scale terrain effects, multipath prediction and the combination of the different aspects yielding more general models.

4.4.1 Semideterministic and empirical models for urban areas

One important output of COST 231 is the development of outdoor propagation models for applications in urban areas at 900 and 1800 MHz bands. Based on extensive measurement campaigns in European cities, COST 231 has investigated different existing models and has created new propagation models. These models, valid for flat terrain, are based on the approaches of Walfisch-Bertoni [24], Ikegami [48] and Hata [49].

COST 231 - Hata-Model

Path loss estimation is performed by empirical models if land cover is known only roughly, and the parameters required for semi-deterministic models cannot be determined. Four parameters are used for estimation of the propagation loss by Hata's well-known model: frequency f, distance d, base station antenna height h_{Base} and the height of the mobile antenna h_{Mobile}. In Hata´s model, which is based on Okumura´s various correction functions [50], the basic transmission loss, L_b, in urban areas is:

$$L_b = 69.55 + 26.16 \cdot \log\frac{f}{MHz} - 13.82 \cdot \log\frac{h_{Base}}{m} - a(h_{Mobile}) + (44.9 - 6.55 \cdot \log\frac{h_{Base}}{m}) \cdot \log\frac{d}{km} \quad [1)] \qquad (4.4.1)$$

where:

---

1) "log" means "$\log_{10}$"

$$a(h_{Mobile}) = (1.1 \cdot \log \frac{f}{MHz} - 0.7)\frac{h_{Mobile}}{m} - (1.56 \cdot \log \frac{f}{MHz} - 0.8) \quad (4.4.2)$$

The model is restricted to:

f :	150 ... 1000 MHz
h_{Base} :	30 ...200 m
h_{Mobile}:	1 ...10 m
d :	1 ...20 km

COST 231 has extended Hata´s model to the frequency band 1500 $\leq$ f(MHz) $\leq$ 2000 by analysing Okumura´s propagation curves in the upper frequency band. This combination is called "COST-Hata-Model" [51]:

$$L_b = 46.3 + 33.9 \log \frac{f}{MHz} - 13.82 \log \frac{h_{Base}}{m} - a(h_{Mobile})$$

$$+ (44.9 - 6.55 \log \frac{h_{Base}}{m}) \log \frac{d}{km} + C_m \quad (4.4.3)$$

where $a(h_{Mobile})$ is defined in equation (4.4.2) and

$$C_m = \begin{cases} 0 \text{ dB} & \text{for medium sized city and suburban} \\ & \text{centres with medium tree density} \\ 3 \text{ dB} & \text{for metropolitan centres} \end{cases} \quad (4.4.4)$$

The COST-Hata-Model is restricted to the following range of parameters:

f :	1500 ... 2000 MHz
h_{Base} :	30 ... 200 m
h_{Mobile} :	1 ... 10 m
d :	1 ... 20 km

The application of the COST-Hata-Model is restricted to large and small macro-cells, i. e. base station antenna heights above roof-top levels adjacent to the base station. Hata´s formula and its modification must not be used for micro-cells.

COST 231 - Walfisch-Ikegami-Model

Furthermore COST 231 proposed a combination of the Walfisch [24] and Ikegami [48] models. This formulation is based on different contributions from members of the "COST 231 Subgroup on Propagation Models" [51]. It

is called the COST-Walfisch-Ikegami-Model (COST-WI). The model allows for improved path-loss estimation by consideration of more data to describe the character of the urban environment, namely

- heights of buildings h_{Roof},
- widths of roads w,
- building separation b and
- road orientation with respect to the direct radio path φ.

The parameters are defined in Figs. 4.4.1 and 4.4.2. However this model is still statistical and not deterministic because only characteristic values can be inserted and no topographical data base of the buildings is considered.

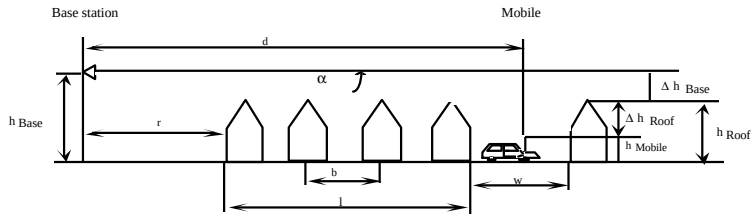

Fig 4.4.1 Typical propagation situation in urban areas and definition of the parameters used in the COST-WI model and other Walfisch-type models [24], [45], [52].

The model distinguishes between line-of-sight (LOS) and non-line-of-sight (NLOS) situations. In the LOS case -between base and mobile antennas within a street canyon - a simple propagation loss formula different from free space loss is applied. The loss is based on measurements performed in the city of Stockholm:

$$L_b(\mathrm{dB}) = 42.6 + 26\log(d/\mathrm{km}) + 20\log(f/\mathrm{MHz}) \quad \text{for } d \geq 20 \text{ m} \tag{4.4.5}$$

where the first constant is determined in such a way that L_b is equal to free-space loss for d = 20 m. In the NLOS-case the basic transmission loss is composed of the terms free space loss L_0, multiple screen diffraction loss L_{msd}, and roof-top-to-street diffraction and scatter loss L_{rts}.

$$L_b = \begin{cases} L_0 + L_{rts} + L_{msd} & \text{for } L_{rts} + L_{msd} > 0 \\ L_0 & \text{for } L_{rts} + L_{msd} \leq 0 \end{cases} \tag{4.4.6}$$

The free-space loss is given by

$$L_0(\mathrm{dB}) = 32.4 + 20\log(d/\mathrm{km}) + 20\log(f/\mathrm{MHz}) \tag{4.4.7}$$

The term L_{rts} describes the coupling of the wave propagating along the multiple-screen path into the street where the mobile station is located. The determination of L_{rts} is mainly based on Ikegami's model. It takes into account the width of the street and its orientation. COST 231, however, has applied another street-orientation function than Ikegami:

$$L_{rts} = -16.9 - 10\log\frac{w}{\mathrm{m}} + 10\log\frac{f}{\mathrm{MHz}} + 20\log\frac{\Delta h_{Mobile}}{\mathrm{m}} + L_{Ori} \tag{4.4.8}$$

$$L_{Ori} = \begin{cases} -10 + 0.354\frac{\varphi}{\mathrm{deg}} & \text{for } 0° \le \varphi < 35° \\ 2.5 + 0.075(\frac{\varphi}{\mathrm{deg}} - 35) & \text{for } 35° \le \varphi < 55° \\ 4.0 - 0.114(\frac{\varphi}{\mathrm{deg}} - 55) & \text{for } 55° \le \varphi < 90° \end{cases} \quad 1) \tag{4.4.9}$$

$$\Delta h_{Mobile} = h_{Roof} - h_{Mobile} \tag{4.4.10}$$

$$\Delta h_{Base} = h_{Base} - h_{Roof} \tag{4.4.11}$$

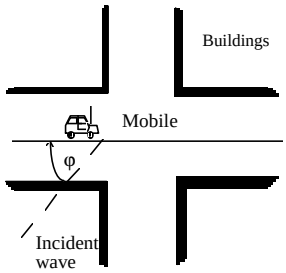

Fig 4.4.2 Definition of the street orientation angle φ.

Scalar electromagnetic formulation of multi-screen diffraction results in an integral for which Walfisch and Bertoni published an approximate solution in the case of base station antenna located above the roof-tops. This model is extended by COST 231 for base station antenna heights below the roof-top

---

1) L_{ori} is an empirical correction factor gained from only a few measurements

levels using an empirical function based on measurements. The heights of buildings and their spatial separations along the direct radio path are modelled by absorbing screens for the determination of L_{msd}:

$$L_{msd} = L_{bsh} + k_a + k_d \log\frac{d}{km} + k_f \log\frac{f}{MHz} - 9\log\frac{b}{m} \qquad (4.4.12)$$

where

$$L_{bsh} = \begin{cases} -18\log(1+\frac{\Delta h_{Base}}{m}) & \text{for } h_{Base} > h_{Roof} \\ 0 & \text{for } h_{Base} \le h_{Roof} \end{cases} \qquad (4.4.13)$$

$$k_a = \begin{cases} 54 & \text{for } h_{Base} > h_{Roof} \\ 54 - 0.8\frac{\Delta h_{Base}}{m} & \text{for } d \ge 0.5 \text{ km and } h_{Base} \le h_{Roof} \\ 54 - 0.8\frac{\Delta h_{Base}}{m}\ \frac{d/km}{0.5} & \text{for } d < 0.5 \text{ km and } h_{Base} \le h_{Roof} \end{cases} \qquad (4.4.14)$$

$$k_d = \begin{cases} 18 & \text{for } h_{Base} > h_{Roof} \\ 18 - 15\frac{\Delta h_{base}}{h_{roof}} & \text{for } h_{Base} \le h_{Roof} \end{cases} \qquad (4.4.15)$$

$$k_f = -4 + \begin{cases} 0.7(\frac{f/MHz}{925} - 1) & \text{for medium sized city and suburban} \\ & \text{centres with medium tree density} \\ 1.5(\frac{f/MHz}{925} - 1) & \text{for metropolitan centres} \end{cases} \qquad (4.4.16)$$

The term k_a represents the increase of the path loss for base station antennas below the roof tops of the adjacent buildings. The terms k_d and k_f control the dependence of the multi-screen diffraction loss versus distance and radio frequency, respectively. If the data on the structure of buildings and roads are unknown the following default values are recommended:

h_{Roof} = 3 m x { number of floors } + roof-height

$$\text{roof - height} = \begin{cases} 3 \text{ m pitched} \\ 0 \text{ m flat} \end{cases}$$

$b = 20 \ldots 50$ m

$w = b / 2$

$\varphi = 90°$

The COST-WI model is restricted to:

f :	800 ... 2000 MHz
h_{Base} :	4 ... 50 m
h_{Mobile} :	1 ... 3 m
d :	0.02 ... 5 km

The model has also been accepted by the ITU-R and is included into Report 567-4. The estimation of path loss agrees rather well with measurements for base station antenna heights above roof-top level. The mean error is in the range of $\pm$3 dB and the standard deviation 4-8 dB [53], [54]. However the prediction error becomes large for $h_{Base} \approx h_{Roof}$ compared to situations where $h_{Base} >> h_{Roof}$. Furthermore the performance of the model is poor for $h_{Base} << h_{Roof}$. The parameters b, w and φ are not considered in a physically meaningful way for micro-cells. Therefore the prediction error for micro-cells may be quite large. The model does not consider multipath propagation and the reliability of pathloss estimation decreases also if terrain is not flat or the land cover is inhomogeneous.

Comparison with other models

Saunders and Bonar [52], [39] as well as Bertoni and Xia [24], [56], [45], [57] published different closed-form solutions for L_{msd} which are applicable for all values of base station antenna heights. Several papers compare the different approaches with measurements [53], [39], [54], [58], [59], [60].

The results, however, differ markedly depending on the situation, where the models are applied. This effect can be explained by the different validity limits of the different approaches. The Walfisch-Bertoni-Model supposes a high base station antenna ($h_{Base} > h_{Roof}$). The COST-Walfisch-Ikegami-Model is valid for base station antenna heights below 50 m and gives reasonable agreement with measured values for $l > d_S$ (see Fig. 4.4.1), where d_S is called the "settled-field"- distance [53], [61]:

$$d_s = \frac{\lambda d^2}{\Delta h_{Base}^2} \qquad (4.4.17),$$

where λ is the wave length in m. The case $l < d_s$ covers grazing incidence, where the COST-Walfisch-Ikegami-Model is poor. On the other hand Saunder's Flat-Edge-Model covers grazing incidence as long as the condition $r >> l$ is fulfilled. Furthermore the COST-Walfisch-Ikegami-Model and an approach of Maciel et. al [57] include corrections for taking into account the street orientation at the mobile. In [58], [59] an adaptive combination of the different approaches is used in urban macro-cells at 1800 MHz, yielding better results than each of the single models.

4.4.2 Influence of vegetation

A few papers within COST 231 investigated propagation models for wooded environments in the 900 and 1800 MHz bands. A comparative study [62] has been done in Finland applying the Okumura-Hata-Model (945 MHz), the COST-Hata-Model (1807 MHz) and the Blomquist-Ladell-Model [55] (both frequencies) to forested terrain. The Finnish experiments revealed that Hata's model can be used for path loss estimation, except for wet forests at 1800 MHz where an additional path loss of about 5 dB has to be taken into account. Middle European forests containing denser and higher trees than typical nordic woods result in larger additional attenuation. In two other papers [59], [63] forest is modelled as a dielectric layer dividing the two layers air and ground. The path loss is computed based on Tamir's lateral approach [64] yielding reasonable results at 947 MHz and 1800 MHz.

4.4.3 Modelling of large-scale terrain variations

Different methods have been investigated to describe diffraction and forward-scattering processes in inhomogeneous terrain, i.e. the effect of the large-scale variation of the terrain. A rough classification of the methods is given by numerical solutions and approximations (see Tab. 4.4.1).

Numerical solution.

Two terrain-based propagation models for vertically polarised radio waves are described, based on the field integral equation for a smooth surface. The model developed by Aalborg University [65] is based on the Magnetic-Field-Integral-Equation (MFIE) assuming a 2D landscape with no transverse variations, no backscattering and a perfectly magnetically conducting surface (a soft surface). Under these assumptions the method is exact. The method requires only forward integration summing up the contributions

from all previous segments. No attempts have been made to reduce computation time, but the method is well suited as a reference for more approximate methods.

classification	models
numerical solutions	**integral equation methods (IEM):** - magnetic field integral equation (MFIE) [65] - electric field integral equation (EFIE) [66] **parabolic equation methods (PEM):** - FFT multiple half-screen method [67] - parabolic differential equation method [68]
approximations (including ray-optical approaches)	**high-frequency asymptotic methods** - uniform theory of diffraction (UTD)[69] **semi-empirical models** - forward-scattering algorithm (FSA) [70] - Hata + knife-edge diffraction [71], [72] **empirical models** - Hata [49] - neural network approach [73], [74]

Tab. 4.4.1 Methods to consider large-scale terrain variations.

A faster numerically exact approach based on the natural basis method applied to the Electric-Field-Integral-Equation (EFIE) is suggested by the Trinity College Dublin [66]. In this approach a moment method using a novel set of complex basis functions is used, reducing the resulting matrix by a factor of m^2 and its direct solution by a factor of m^3. The basis set has been applied to undulating terrain with distances up to 10 km. For frequencies of 143.9 MHz to 1900 MHz m has ranged from 90 to 600. However, the method to reduce the computational complexity is not restricted to the EFIE but can be applied to any IE, where the unknown current density has to be calculated. Both forward and back scattering are included.

Two methods mainly based on parabolic integral equations are proposed by Berg to build new macro-cell models. The first (heuristic) method [68] is based on the parabolic heat or diffusion equation. The multiple knife-edge approach is used to determine the path loss in non-flat terrain. The equation is solved by using the simple explicit Forward-Difference method. The grid distances are 100 m in the main propagation direction and 5m in height direction in the 900 MHz band. The second method is called FFT-multiple halfscreen diffraction model [67]. The terrain profile is replaced with a number of absorbing half-screens similar to an approach described in [24]. This computational method is also very similar to the SIP procedure [37, 38,

174]. Hence the propagation is described as a multiple diffraction phenomenon where reflections are neglected. The diffracted scalar field is determined using the scalar Helmholtz parabolic integral equation. For the considered situation the Helmholtz integral can be expressed as a convolution which can be solved in a computational efficient way by application of FFT (Fast Fourier transform) techniques.

Ray-optical methods and approximations

In planning a GSM-network the empirical model by Okumura-Hata is still the most used, due to its simplicity. Therefore many variations of Okumura-Hata-based approaches have been investigated [71], [72], where Hata´s path loss is combined with multiple-knife-edge diffraction models. Different methods to determine the effective base station antenna height and terrain undulation correction factors have been considered.

A new ray-optical method [69] is based on the Uniform Theory of Diffraction (UTD). For the ray path calculation with UTD, obstacles along the terrain profile have to be represented by simple geometrical objects. An approximation of the terrain profile is obtained by substituting the terrain obstacles by wedges and convex surfaces. For these objects, expressions exist to compute the UTD diffraction coefficients. For efficient computation, an algorithm for the multiple diffraction calculation is derived using a matrix formulation. Forward-scattering processes are considered heuristically [75] using a two-ray approach. This two-ray approach yields an additional path loss of 20 dB/decade if the distance between Tx and Rx exceeds a so-called breakpoint distance.

In [70] a fast forward-scattering algorithm (FSA) based on empirical propagation curves and geometrical diffraction [76] has been developed. The diffraction algorithm is able to handle up to 15 knife-edges. Measurements in the frequency range 919-1843 MHz have been used for verification. A comparison with a PEM-method [77] revealed prediction errors in the same range for the FSA and the PEM.

Another more empirical method is based on neural network training [73], [74]. The training of the network can be done either by theoretical methods like UTD or by measurements. The decisive advantage of this method is the possibility of deriving training patterns directly from measurements. This allows the system to become very flexible and adapt to arbitrary environments. The training is time consuming, but once the network is trained, the results are obtained immediately. This is supported by the highly parallel structure of the processing.

Comparison of different models.

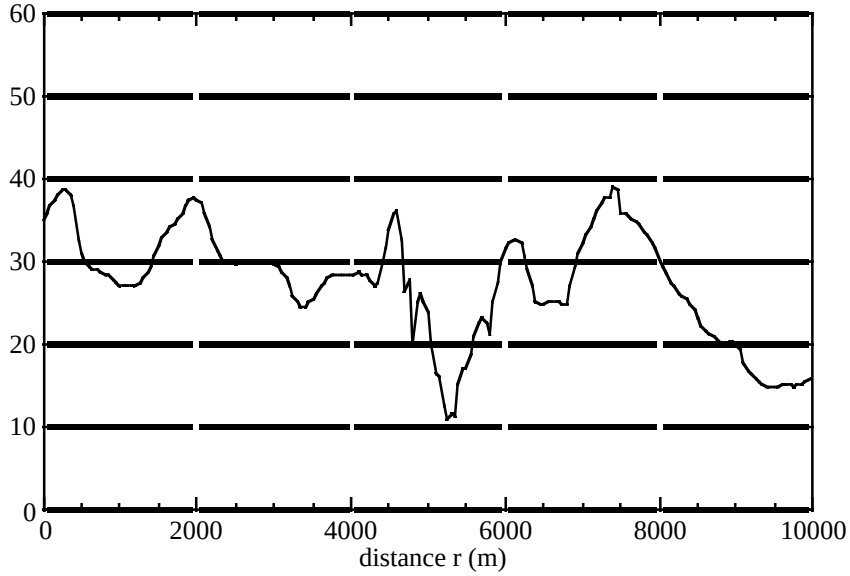

Fig 4.4.3 Terrain profile at "Hjorringvej".

The prediction models are compared to each other and with measurements [65] at different frequencies from 144.9 MHz to 1900 MHz used on five different terrain profiles in rural Denmark. The measurements have been carried out with a transmitter height of 10.4 m and the receiving antenna was 2.4 m above the profile. Polarisation was vertical for both antennas. Path lengths were of 6-11 km along roads being fairly straight over for the distance where the profiles are examined. This gives a good approximation of the 2D assumption within the above described models. The height variations are in the order of 20-50 m and only a few trees or buildings are along the profiles. Fig. 4.4.3 shows one of the profiles at "Hjorringvej".

A comparison of predictions (MFIE-method) with the measurements is depicted in Fig. 4.4.4 (970 MHz) and Fig. 4.4.5 (1900 MHz). Tab. 4.4.2 presents the numerical mean error and standard deviation for seven different models at the frequencies 970 MHz and 1900 MHz. More detailed results comparing these measurements also at other frequencies and with additional models can be found in the literature [67], [71], [75], [78]-[80].

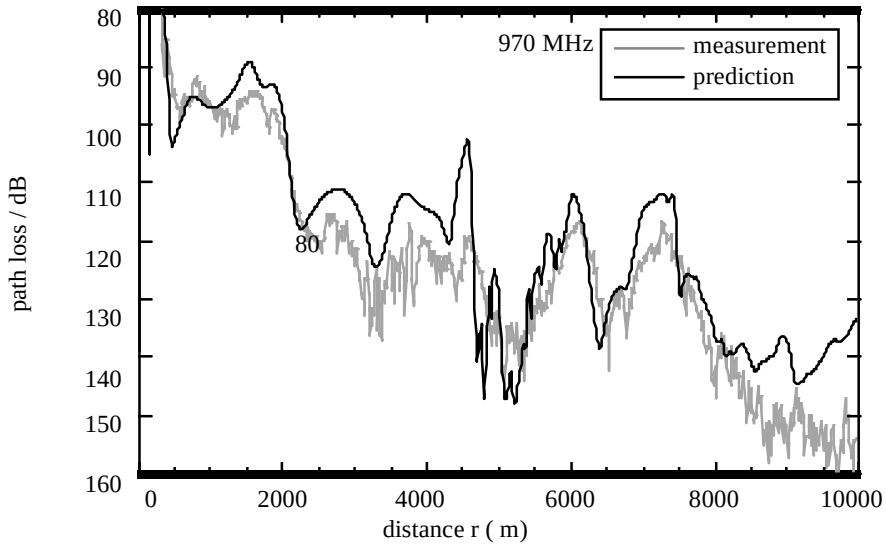

Fig 4.4.4 Measurement and prediction by the MFIE-method for the terrain profile "Hjorringvej" at 970 MHz.

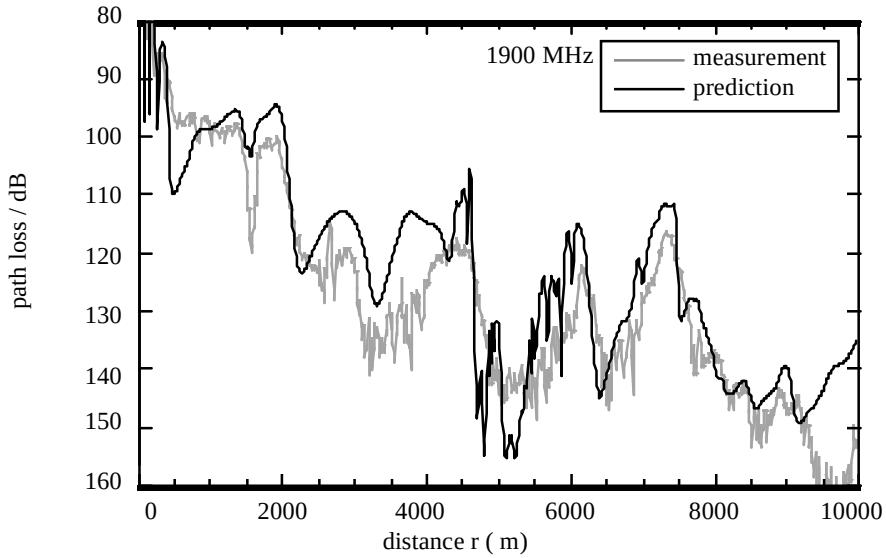

Fig 4.4.5 Measurement and prediction by the MFIE-method for the terrain profile "Hjorringvej" at 1900 MHz.

model	mean /dB 970 MHz	STD/dB 970 MHz	mean/dB 1900 MHz	STD/dB 1900 MHz
MFIE	5,5	6,3	5,1	8,7
IFIE	*)	6,5	*)	8,2
FFT-multiple half-screen	1,7	6,1	3,0	7,6
Parab. diff. FD-Method	3,0	5,4	6,7	8,3
UTD	6,2	8,9	3,4	10,2
Neural Network	2,9	5,7	*)	*)
Hata	2,8	9,0	4,0	10,3
FSA	5,0	6,0	5,3	6,8

*)values are not available

Tab. 4.4.2 Comparison of different propagation models; numerical mean values and standard deviations derived from 5 terrain profiles (at 970 MHz from 4 profiles only).

4.4.4 Estimation of time dispersion

This section addresses the prediction of multipath signals. Emphasis is placed on automatic detection of long excessive time dispersions. An overview is given over approaches and results from COST 231 participants. The task of predicting multipath signals can be subdivided into two subsequent steps. The first step consists of an algorithm to extract the relevant scattering areas. All known approaches take into account single-scattering processes only. Every potential scatter area has to fulfil the LOS-condition to both Tx and Rx. In a second step the path loss for each multipath signal has to be calculated. This calculation consists of mainly three parts:

- propagation from transmitter to the scattering surface,
- process of scattering at the surface,
- propagation from the scattering surface to the receiver,

The various models differ both in terms of the algorithms to determine the scattering areas and on the methods to determine the path loss.

The IHE-model from the University of Karlsruhe [63], [69], [75], [81] is intended to be a complete propagation simulation model for rural areas. To describe the scattering process the bistatic polarimetric scattering matrix, depending on land usage terrain classes and on the angle of incidence and both scattering angles is applied. The average bistatic cross section matrix

derived by the method of small perturbation and by the Kirchhoff method is used. Both coherent and incoherent scattering are considered in the model. The determination of the scatterer location is often a time consuming process. In [82] fast scatterer search algorithms are suggested. Large improvements are obtained saving 80-90% of computing time compared to traditional methods. A comparison between measured and predicted locations of interfering scatterers is made in [83] at a frequency of 225 MHz (Digital Audio Broadcasting). In general the agreement is satisfactory, although multiple scattering near the antennas and surroundings gave some errors.

The University of Vienna uses path tracing [84] as a practical technique for the identification of areas of heavy time dispersion based on systematic ray tracing and weighting of the paths that the power can take from transmitter to receiver. Single reflections are considered and modelled as an area element radiating isotropically to half space. Between transmitter, scatterer and receiver (quasi) free space propagation is assumed. The model is prepared and planned to be expanded to study consideration of important single scatterers.

In Davidsen's approach [85], [86] multipath propagation is modelled with single-scatter paths. Scattering is modelled as a diffuse Lambert surface. Terrain data is approximated by relatively few planes taken from maps. The planes are subdivided into area elements that are the basis of the calculation. Propagation over sea-water in fjords is studied carefully finding that scattering due to the microstructure (ripple, foam and spray) of the sea is negligible compared with line-of-sight, whereas power scattered by the macrostructure (large scale, roughly periodic waves) is significant.

The model of Deutsche Telekom [87]-[89] is based on channel sounder measurements in hilly terrain. Based upon these measured impulse responses an approach is suggested extending an existing 2D model by additional single-scatter paths. The path loss for the propagation from the transmitter to the scattering and from there to the receiver is assumed to be free space loss. Furthermore the assumption is made that the scattering area acts as a Lambert transmitter. The scattering parameter C is extracted from the measurements. It is shown that 10 log C = -10 dB in the 900 MHz band (10 log C = -13 dB in the 1800 MHz band) provides a good fit to the measurements. An example for a measured and predicted scattering function is displayed in Fig. 4.4.6.

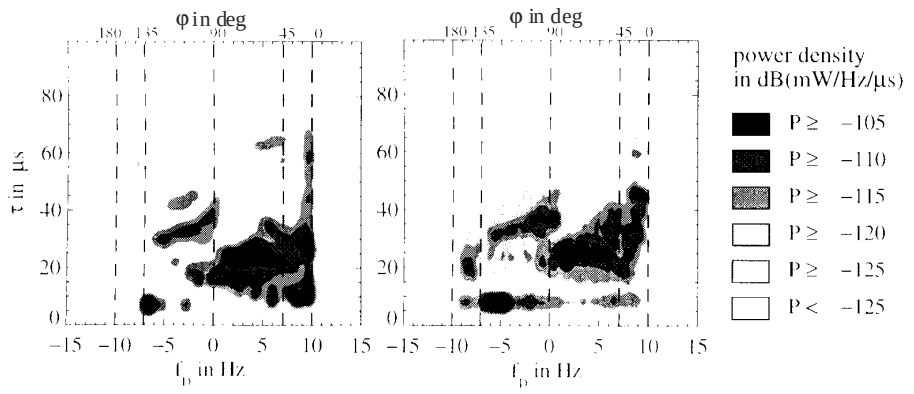

Fig 4.4.6 Measured (right) and predicted (left) scattering functions using the Telekom model.

In Fig. 4.4.6, φ denotes the incidence angle of the signal components with respect to the direction of the moving mobile. τ is the time delay and f_D the Doppler-shift.

For the future channel sounder measurements will be useful to determine both empirical parameters C and bistatic scattering cross sections for different types of terrain. All the models can also be used to predict the propagation system parameters, e.g. delay spread or Q_{16}. In [90] and [91] it is shown how the relevant parameters can be derived from a 3D prediction model.

4.4.5 General models

Some new general models for estimation of path loss in macro-cells have been proposed using topographical and land usage data in resolutions from 50 m x 50 m to 250 m x 250 m.

The main idea of Vodafone´s method [25], [92] is to reduce the details of path profiles to simple geometrical shapes, e. g. wedges or cylinders, and to apply additionally empirical correction factors. Losses from the free space field strength are calculated for ground reflection and diffraction, ground cover along the path and for clutter from the canopy height down to the mobile. The model is verified by an extensive measurement campaign revealing a standard deviation of about 8 dB in the 900 MHz band using a 250 m x 250 m database.

The IHE-rural-model with receiver near range extension [63], [75] incorporates typical macro situations for forested and urban areas in order to

determine additional path loss caused by land usage. In the case of an urban environment the additional path loss is determined by means of the UTD, whereas in forested areas the above described lateral wave approach is applied. The extension is also used for the multipath signals yielding reasonable agreement with both wideband and narrowband measurements in a GSM 900-network, see Fig. 4.4.7.

A hybrid propagation model for prediction of DCS 1800 macro-cells is proposed by E-Plus [58], [59]. The model is based on a "unit construction system" , combining different models, e. g. COST-Walfisch-Ikegami, flat edge [52], [39] and Maciel [45] in urban areas. The prediction system consists of several modules which are selected according to practical and theoretical criteria. The switching of the modules is completely unsupervised and the computing time for the full prediction of an area of 30 km x 30 km is only 5 min on a SunSparc20 workstation. The model is verified by numerous measurements in the E-Plus-network in different landscapes in Germany, including urban, rural, flat, hilly and mountainous terrain. A typical RMS error of 6-9 dB is achieved in all areas.

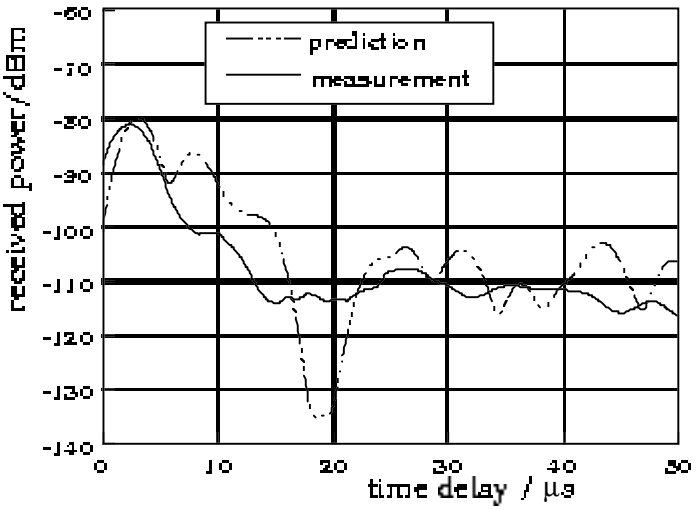

Fig 4.4.7 Measured and predicted impulse responses in a hilly terrain using the IHE-receiver-near-range model at 947 MHz. For the predicted impulse response the filter characteristic of the receiver is taken into account using the algorithms published in [90].

4.5 Propagation Models for Small- and Micro-Cells

Dieter J. Cichon , IBP Pietzsch KIH Group, Germany

4.5.1 General

The design and implementation of personal communications systems requires the prediction of wave propagation relating to signal-to-noise and signal-to-interference calculation in a cellular system [93]. Small-cell network configurations - especially micro- and pico-cell types - are of major interest for urban environments. The commonly used criteria for the definition of a micro-cell is related to the base-station height. For a typical micro-cell the base-station antenna height is below the average roof-top level of the surrounding buildings or at about the same height. Thus the resulting cell radius is in the range of about 250-500 m. However a prediction range of up to several km has to be regarded for inter-cellular interference calculations. A pico-cell base-station is usually installed inside a building providing coverage also outside around the building. A tutorial and overview on wave propagation modelling for wireless personal communications is given in [94].

The propagation models developed in COST 231 are based on theoretical and empirical approaches. Ray optical methods with either simplified analytical solutions or pure ray tracing techniques have been proposed. The availability and usage of proper urban terrain data bases, as described in Sec. 4.1, in combination with ray tracing methods (see Sec. 4.5.4) enables site-specific propagation modelling for the prediction of path loss and time spreading of the signal; the latter has a major impact on the performance of digital radio systems.

Radio transmission in urban environments is subject to strong multipath propagation. To consider these effects in a propagation model, it is necessary to gain knowledge of all dominant propagation paths. These paths depend primarily on the base station height with respect to the building heights around. A study on micro-cellular multipath propagation effects with respect to DECT-system performance is given in [95]. For simplification of propagation modelling several two-dimensional models have been developed under the assumption of infinitely high buildings (see Sec. 4.5.2). Hence these models only take into account wave propagation around buildings. As a result, computation-time efficient, analytical path loss models have been derived considering simple building geometries. In case

of low building heights, over-roof-top propagation have to be regarded, too (see Sec. 4.5.3). Analytical approaches and simple models with empirically based extensions and modifications are given in, e.g., [24], [48], [51], [45], [60].

The second group of small-cell models allow a very site-specific, three-dimensional path loss and signal spread prediction for base-station heights below as well as at about roof-top level of the buildings (see Sec. 4.5.4). Hence, not only the shape but also the height of a building has to be incorporated. Of course, due to the three-dimensional ray tracing these models require a higher computation-time than the simplified approaches mentioned above.

The micro-cell models are generally valid only for flat urban area. Investigations on the influence of terrain on micro-cell propagation are presented in, e.g. [94] and [96]. Further on the effects of urban-type vegetation (like line-up trees, parks, etc.) on radio propagation [92] are not included in these micro-cell models. Both aspects are of great interest from an engineering point of view and should be regarded in further developments of these models.

4.5.2 Two-dimensional models for below roof-top propagation

Uni-Lund model

Micro-cellular path loss prediction is performed by two separate models for LOS and NLOS, respectively [97], [98]. Both models are based on the properties of free space propagation; all model parameters are empirically gained.

The LOS model describes the dual-slope behaviour [94] of the path loss, where the first part is a power function (decay index $n \approx 2$) of the Tx-Rx distance d. At the break-point distance d_B the power decay increases (decay index $n \approx 4$). The corresponding power decay indices n_1 and n_2 depend on the urban environment, thus they have to be gained by path loss measurements to be performed in the prediction area. For NLOS propagation the model is based on the observation that there is a short distance at the corner where the signal level is still of the same magnitude as in LOS. Further down the street there is a rapid increase of loss until finally the signal strength decreases with about $n \approx 2.5\text{-}3.0$.

Ericsson micro-cell model

This model is based on a mathematical method for path loss prediction, which is recursive, reciprocal, very simple, and computation-time efficient [99]. Loss is determined along paths following the different streets, thus this method is suitable for ray tracing techniques. The approach is not restricted to perpendicular street crossings. It can handle arbitrary angle of crossing streets as well as bent streets with linear segments. The model approach is based on the well known expression for path loss between two isotropic antennas, where the physical distance is replaced by an imaginary distance, which is defined by a recursive expression as a function of the number of nodal points and corresponding street orientation angles of the path between transmitter and receiver. The dual-slope behaviour [94] of the distance dependence of the path loss is also included in the proposed model. In addition, the distance dependence of the COST-WI model is applied to consider over-roof-top propagation in case of NLOS.

CNET micro-cell model

This model is based on an analytical, semi-deterministic approach for the consideration of reflected and diffracted waves [100]. Only below roof-top propagation around buildings and street crossings with four corners are regarded. The angle of crossing streets can be arbitrary. Nine reflections in a LOS case and nine reflections in a following NLOS case are included. Ground reflections and street corner diffraction between the line-of-sight and the non-line-of-sight street are regarded as well. The Uniform Theory of Diffraction is used for the street corner diffraction calculation, wherein the finite conductivity of the walls is introduced through heuristic coefficients.

Swiss Telecom PTT micro-cell ray tracing model

Micro-cell environments are described by a two-dimensional layout of buildings which are given to the software program in terms of vectors defining the building walls. Arbitrary two-dimensional building geometry can be handled. Additionally, the permittivity and conductivity of each building wall can be considered if available. In operational use the electrical characteristics are usually taken to be the same for all buildings in a given area. Specular reflection and diffraction are the propagation phenomena taken into account [101]. Ground reflection, scattering and over-roof-top propagation which are expected to dominate in areas far from the transmitter are neglected so far. The software computes all reflected and diffracted rays up to some predetermined order. This is performed according to an efficient implementation of the image theory which takes advantage of the assumed

fact that rays do not traverse the buildings. To take into account the diffraction effects, virtual sources are placed on all building corners viewed by other images and virtual sources. All image and virtual point sources are generated up to a given order starting from the original source at the base-station antenna location. The image and virtual sources are then used to trace all combinations of reflected and diffracted rays. The path loss is derived by superposition of all rays at the receiver location. Alternatively the channel impulse response can be evaluated by considering the magnitude, phase and delay of each ray.

Uni-Karlsruhe model 2D-URBAN-PICO

A ray launching approach for two-dimensional prediction of wave propagation in micro-cells, including indoor coverage, is proposed in the 2D-URBAN-PICO model [4], [102], [103]. This approach takes into account multiple reflected and multiple wall-penetrated ray paths as well as combinations of multiple reflected/penetrated ray paths. The urban environment is two-dimensionally described by an arbitrary number of walls, or further windows, doors, etc., each defined by its position and type. Building walls are modelled as multi-layered media given by thickness, permittivity and tang loss factor. At the transmitter location a certain number of rays are successively launched in discrete directions, which are equally distributed over 2π within the horizontal propagation plane. When the central ray of a ray tube intersects with an obstacle, the incident ray is decomposed into a specularly reflected and a penetrated ray. Both rays are propagating to the next intersection, where the decomposition process is repeated. This procedure is continued until a predetermined number of intersections is reached. A ray-splitting algorithm is used to restrict the maximum divergence of each ray. Reception is determined according to Fig. 4.7.3 in Sec. 4.7.5.

TLM based model

A technique similar to the so-called transmission line matrix (TLM) is applied for the propagation modelling in urban micro-cells. This method is based on a direct discretisation of the building layout onto a two-dimensional lattice. The TLM based method can be assimilated to the so-called Lattice Boltzmann Models (LBM), which describes a physical system in terms of the motion of fictitious microscopic particles on a lattice. A natural implementation of wave propagation dynamics within the framework of the LBM approach is provided by the TLM method. According to the Huygens principle, a wave front consists of a number of spherical wavelets emitted by secondary radiators. The TLM method used here is a discrete

formulation of this principle. For this purpose, space and time are represented in terms of finite, elementary units Δr and Δt. LBM are characterised by a simultaneous dynamics and a very simple numerical scheme suitable for very efficient implementations on massively parallel computers [21]. The interpretation of the dynamics in terms of flux makes the boundary conditions easy to implement. The relationships with conventional electromagnetic TLM methods remain to be examined in details.

Assuming infinite building height, the raw simulation results of the TLM based method implies a two-dimensional propagation (a cylindrical source problem). The results are converted to three-dimensional propagation consideration (point source problem) by computing a renormalisation of the predicted results according to the distance between transmitter and receiver. An additional, although simpler, re-normalisation is used to convert to the desired frequency the simulated frequency resulting from the chosen grid size of the lattice.

Telekom micro-cell model

A network of street canyons connected via the street crossings is used as standard geometrical configuration for path loss calculation. A limited set of parameters and some empirical simplifications and approximations are used. Three categories of propagation are regarded: LOS, NLOS to a perpendicular street, and NLOS to a parallel street [27]. Latter one includes also a over-roof-top propagation term according to Walfisch-Bertoni [24]. The applicability of this model is confined primarily in dense urban environments where street canyons can be assumed.

4.5.3 Two-dimensional models for over-roof-top propagation

COST-Walfisch-Ikegami model

(==> see Section 4.4)

Uni-Valencia model

The basic approach is to separate the propagation effects into "over-roof-top propagation" and "3D multipath effects in the mobile neighbourhood". A modified Walfisch-Bertoni model for description of over-roof-top propagation is applied [60]. The restriction for the incidence angle and for the "final building diffraction" angle have been eliminated [105]. Latter one has been empirically gained, however its value is very close to the theoretical solution for a 90^{o} wedge. The empirical approach is due to the

fact that digital building maps or vector data, i.e., do not provide information about the roof-top shape, thus a theoretical expression cannot be applied, appropriately.

First and 2nd order propagation mechanisms are considered for a Tx-Rx link. It is assumed that incident rays at Rx are scattered at elements (wall, wedge, etc.) which are in LOS to Rx. These Rx-neighbourhood scatter elements are determined by application of a simple ray tracing algorithm. The incidence fields at those elements are calculated by the 2D model mentioned above [106]. Three parameters are used to describe the properties of the scatter elements as there are: Percentage of flat surface, correlation distance, standard deviation of the roughness; default values are 60 %, 3 m and 40 cm, respectively.

For applications in micro-cell environments, the ray tracing algorithm for the 3D model has to be modified to consider at least 3rd order contributions, too. In case Tx is below the mean roof-top level, a third part of the model appears, which is simply described as an additional diffraction loss (2D approach) and/or by applying the above 3D multipath model to the Tx-neighbourhood. Of course, the additional base station diffraction loss and multipath terms depend on the Rx position.

Swiss Telecom PTT over-roof-top model

A pathloss prediction software designed for flat or hilly urban areas has been developed at the Swiss TELECOM PTT. The software (called MCOR) implements multi-knife edge propagation computations over radials launched from the base station.

The propagation model is based on Deygout's approximation to compute multi-knife edge diffraction [107]. The Deygout method is modified according to the concepts presented by VODAFONE [92]. This modification mitigates the linear increase of the path loss due to multiple diffraction in the original Deygout method. The algorithm suggested by VODAFONE decreases the diffraction effects by reducing successive diffraction coefficients in dB by 1/2, 1/4 and 1/8. Inspired from this idea, this model decreases the diffraction effects on each side of the so-called main edges simply by reducing the diffraction coefficients in dB by $(1/2)^n$, where n is the order of the main edges in the Deygout method. For the results presented here, the maximum level is limited to 4 (n_max = 3), thus a maximum of 15 diffractions are computed. The chosen diffraction coefficient is given by the simple CCIR formula [108]. Another modification is the use of a dual slope model for the reference path loss [109]. For the results presented here, the

parameters of the dual slope model have been fitted from ten calibration points given along a particular measurement route. The buildings have been represented by a single knife-edge placed in the middle of each building, which is determined when constructing the profiles along the radials.

The MCOR computation for the results presented in Sec. 4.5.6 takes about 30 minutes on a Pentium 66 MHz under Windows NT for a prediction of 480 x 680 points with a 5 m resolution (note that the prediction data on the measured routes is then extracted from the prediction matrix over the whole region).

CSELT model

Over-roof-top propagation is regarded in this model, which is based on the Walfisch-Bertoni approach [24] extended by consideration of building heights within the vertical propagation plane. Obstacles (buildings) are treated as half-plane screens, which are perfectly absorbing, infinitely thin in propagation direction and infinitely wide across it. For base stations well above average roof-top height it is assumed that the roof-top to street diffraction at the last obstacle is the dominant loss mechanism affecting the radio link, thus Deygout´s diffraction approach is applied in this model. A digital data base containing position and height of the buildings is used to obtain a site-specific two-dimensional propagation modelling approach [110].

4.5.4 Three-dimensional models for arbitrary base-station heights

The propagation models described in this section are suitable for the prediction of path loss as well as the channel impulse response under consideration of the three-dimensionally described buildings.

CNET ray launching model

The program simulates ray launching in three dimensions. Buildings are represented by polyhedrons. Multiple reflection and diffraction processes are considered in the model [111]. Building penetration, scattering at wall irregularities and diffraction at vertical wedges are neglected in the model. Reflection loss is the only physical parameter to be fitted since diffraction loss is computed from semi-empirical formula.

ASCOM-ETH micro-cell model

To study the propagation in micro-cell, the image source method has been incorporated into a ray-tracing approach for taking into account multiple reflections from the walls and streets [16], [112]. The model used the

detailed three-dimensional description of the environment. This comprises the permittivity and conductivity of the walls and street materials. Complex impulse responses were derived from the model calculations, which were compared to the corresponding wideband measurements. A large number of different real environments have been considered to test the model. Good agreement has been found between the modelled results and the measurements. This enabled a classification into few types of environments covering the physical situations most relevant for urban micro-cells: propagation in lineal urban streets (LOS) and coupling into side streets (NLOS). The transition region between LOS and NLOS has been analysed in much detail, as the channel behaviour under such conditions is very important for wireless communication system design.

Villa Griffone Lab's (VGL) model

The field prediction program developed at the Laboratories of Villa Griffone by the researchers of the University of Bologna and of the Ugo Bordoni Foundation is based on a quasi 3D ray tracing/UTD technique [113]. It can be applied to both macro-cellular and micro-cellular systems and can provide both narrowband coverage prediction and wideband channel estimates. Each city block is represented by a prism having a polygonal base corresponding to the shape of the block and a height corresponding to the average height of the buildings in the block. To each prism the corresponding permeability and conductivity values are associated. The environment is thus described as a set of basic objects such as plane walls or lossy wedges.

A quasi 3D ray tracing procedure is performed including rays within the transverse Tx-Rx plane with multiple reflections on building walls and diffractions on corners, and in addition other significant rays experiencing reflection over terrain are considered. No predefined limit is set to the number of multiple reflections or diffractions experienced by each ray; however, a limit can be provided by the user in order to minimise computation time. The algorithm starts determining the set of objects, which have LOS to the transmitter, resulting in the first level of the "viewed objects" tree. Repeating this LOS-determination procedure under consideration of reflection and diffraction points leads to further levels in the "viewed object" tree; the receiver location is the last tree level. After completion of the tree the actual path of each ray can be determined by means of a backtracking process, and the corresponding contribution to the total received field can be computed by means of reflection and diffraction coefficients [113]. Additionally, the Saunders-Bonar model [52] is used, if

over-roof-top propagation should be regarded, too. Also the attenuation due to vegetation can be considered by means of the Foldy-Twersky method [114] when a vegetation map is available.

Uni-Stuttgart 3D micro-cell model

This is a rigorous three-dimensional modelling approach with possible path finding over the entire solid angle [115], [116]. Buildings are described by a polygon with a set of cartesian co-ordinates and a flat roof-top at constant height. Electrical building parameters can also be stored if available. A ray launching algorithm where rays are launched from a fixed point source in all relevant directions is used for path finding, a UTD approach is used for propagation calculation. At potential receiver locations the field strengths of the incident rays are summed up. Less than three diffraction but up to six reflection processes (for modelling of wave guiding effects) can be regarded in the 3D case. In case of more diffraction processes are required, a 2D prediction approach based on the Walfisch-Ikegami formula is used. Topography can be included by defining triangular surface elements which are treated as potential scatterers [117]. The basic characteristics of this approach are: fast algorithm for area prediction, simultaneous calculation for different receiver heights, and unsuitableness for point to point predictions.

Uni-Karlsruhe model 3D-URBAN-MICRO

A three-dimensional approach for propagation simulations in micro- and macro-cellular cases, where base-stations above as well as below building heights can be considered, is proposed by the 3D-URBAN-MICRO model, developed at the University of Karlsruhe [4], [81], [104], [118]. This model is able to use either grid (pixel) data or vector oriented data containing building shape and building height. For the grid data a reasonable horizontal resolution is about 5-15 m, depending on the urban micro structure and the desired approximation of the building shapes. Building heights are approximately given by the number of floors and corresponding floor height.

From numerous transmitter (Tx) to receiver (Rx) propagation paths, the most dominant ones have to be selected to obtain the total path loss. Roof-top diffracted paths are included in the vertical plane approach, while around building diffracted paths are modelled within the transverse plane approach as depicted in Fig. 4.5.1. The propagation in both the vertical and the transverse plane is two-dimensionally regarded. However, the determination of building corners in the transverse propagation plane is not necessarily performed in a horizontal plane.

Multiple wedge diffraction processes are evaluated by successively computing single wedge diffraction based on the UTD. Additional 3D propagation paths via scattering at ground and building walls are separately regarded. A modified Kirchhoff Method with scalar approximation is applied for surface scattering calculations [4]. Recently, this model has been extended for receiver locations within buildings to provide indoor coverage prediction by outdoor base stations [119].

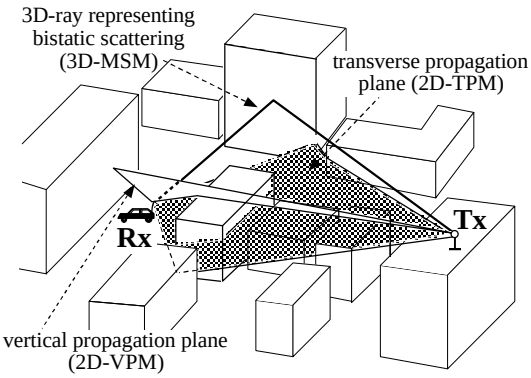

Fig. 4.5.1 Ray tracing within a vertical and a transverse Tx-Rx plane.

4.5.5 Overview over the Prediction Models

The small- and micro-cell propagation models are briefly summarised and listed in the Table 4.5.1 (CIR = channel impulse response).

4.5.6 Comparison with path loss measurements at 947 MHz

A path loss measurement campaign including different base station heights at several locations have been carried out in downtown Munich by the German GSM network operator Mannesmann Mobilfunk GmbH. The performance of some of the introduced models is investigated by comparison with the measurements.

Description of the measurement scenario

Building data in vector format covering an area of about 2.4 x 3.4 km^2 in downtown Munich have been provided by Mannesmann Mobilfunk. Since the selected test site has a fairly flat ground, the topography (which has been also available) is not considered within this study of model performances. Hence, only the two-dimensional building layout with height information of each single building is used by the propagation models.

The resulting building map (based on pixel data) is shown in Fig. 4.5.2, where the absolute terrain heights are grey scale presented. Additionally, the three measurement routes METRO200 (970 points; ground height: 512±4 m, s_h = 2 m), METRO201 (355 points; ground height: 516±2 m, s_h = 1.3 m)

and METRO202 (1031 points; ground height: 514±5 m, s_h = 1.9 m), as well as the transmitter location (Tx) are marked in the map.

prediction model	method	features/restrictions	terrain data	results
Uni-Lund (S)	empirical	BS below roof-top	2D building layout	path loss
CNET micro cell model (F)	analyt. LOS + NLOS model	2D (horizontal plane) + 2D (over-roof-top)	2D building layout	path loss
RT - Swiss Telecom PTT (CH)	ray tracing	2D (horizontal plane)	2D building layout	path loss and CIR
Uni. Geneva / Swiss Telecom PTT(CH)	TLM like	2D (plane)	2D building layout	path loss
2D-URBAN-PICO Uni. Karlsruhe (D)	ray launching	2D (horizontal plane)	2D building layout	path loss and CIR
Telekom (D)	analyt. LOS +NLOS model	2D (horizontal plane) + 2D (over-roof-top)	2D building layout	path loss
Ericsson (S)	ray tracing + COST-WI	2D (horizontal plane) +2D (over-roof-top)	2D building layout	path loss
COST-231 small-cell	Walfisch-Ikegami mod.	2D (over-roof-top)	building classes	path loss
Uni. Valencia (ES)	Walfisch-Bertoni mod.	2D (vertical plane) + 3D reflections at Rx	2D building layout + building height	path loss, FS dis-tribution
MCOR - Swiss Telecom PTT (CH)	modified Deygout	2D (over-roof-top)	2D building layout + building height	path loss
CSELT (I)	Deygout	2D (over-roof-top) BS above roof-top	3D raster data	path loss
CNET ray launching model (F)	ray launching	3D (no diffraction at vertical wedges)	3D building layout	path loss and CIR
ASCOM-ETH (CH)	Ray-tracing by image source	3D, only reflections	2D building layout + building height	path loss and CIR
Villa Griffone Lab, Bologna (I)	ray tracing; Saunders-Bonar	transverse plane + ground reflection; 2D (over-roof-top)	2D building layout + building height	path loss and CIR
Uni. Stuttgart (D)	ray launching + W/I model for 2D case =>	3D (2 diffr. + 6 reflec. processes); 2D (vertical plane)	2D building layout + building height	path loss and CIR
3D-URBAN-MICRO Uni. Karlsruhe (D)	ray tracing	2D (transverse plane) 3D surface scatter	2D building layout + building height or raster data	path loss and CIR

Tab. 4.5.1 Small- and micro-cell prediction models: An overview

Fig. 4.5.2 Munich test site with measurement routes (~ 25 km) and transmitter location; terrain height is grey scaled.

The measurements have been performed at 947 MHz, the transmitter and receiver height is 13 m and 1.5 m above ground, respectively. An approximately 10 m sector average of the measured signal has been converted to path loss and stored with the Rx location, which is at about the centre of the averaging sector.

Performance of the models

The following institutes have participated in this study: CNET (France), CSELT (Italy), Ericsson Radio Systems (Sweden), Swiss PTT/Uni. Geneva (Switzerland), Villa Griffone Laboratories (Italy), University of Karlsruhe (Germany), and University of Valencia (Spain). For calibration purpose, all participants received the measured path loss data of 11 Rx locations selected from the METRO200 route. Except the building data in vector format and all Rx locations, no additional information have been provided to the participants, leading to an almost "blind test" of the above mentioned prediction models discussed in COST 231.

Results are presented in Fig. 4.5.3 - 4.5.5, where the model predictions and the measured path loss versus Rx locations of the 3 routes (total length of about 25 km) depicted in Fig. 4.5.2 are shown. To improve the visualisation quality of the prediction results, the original curves of the CNET, TLM, MCOR, Griffone and Uni-Karlsruhe model have been smoothed to suppress strong fluctuations and therefore to make the single curves better distinguishable. Since the transmitting antenna height h_t is at 13 m above ground, which is below roof-top of most of the buildings within the test site, almost all Rx locations are in NLOS situations, except some peaks which obviously refer to LOS propagation.

Along routes METRO200 (Fig. 4.5.3) and METRO202 (Fig. 4.5.5) the performances of the Swiss PTT MCOR model and Uni-Karlsruhe ray tracing model, both regarding over-roof-top propagation, and the Ericsson model and CNET model, both regarding around and radially over building propagation, are rather good, with a standard deviation of the prediction error in the range of 5.6-8.6 dB (see also Table 4.5.2), although different propagation paths are regarded by these models. These results indicate that the field contributions of both over-roof-top and around building propagation are in some cases of the same order of magnitude at the receiver.

The Walfisch-Bertoni type model of the University Valencia is an extension of the COST-Walfisch-Ikegami (COST-WI) model, hence regarding over-roof-top propagation. Therefore both results show similar behaviour except an offset of about 10 dB and, of course, the much better performance of the Uni-Valencia model in LOS-situations. For the COST-WI model the

parameters describing the built-up structure are estimated to be h_{Roof} = 20 m, w = 13 m and b = 26 m, respectively. Since it is an empirical model, the model parameters should be properly adjusted to reduce the mean error of 10-17 dB; however the standard deviation of the prediction error is in the range of 6-8 dB, which is fairly good for this simple and fast prediction method. The general trend is a good agreement with the measurements obtained by the PTT ray tracing (RT) model. However, for many Rx locations no ray paths could be determined, as can be seen in Fig. 4.5.3, since the model is restricted to a maximum of 4 reflections or to a maximum of 3 reflections and 1 diffraction per ray. The application of the transmission line matrix method for propagation modelling leads to higher prediction errors compared to the other models. Since this is a very new method, the reasons have not been analysed in detail up to now. The application of the three-dimensionally working Villa Griffone and Uni-Karlsruhe models in the above scenario outperforms very well under the circumstance that these models have been developed for arbitrary base station heights; however here the transmitting antenna is placed at 13 m above ground, which is more or less below the average building height in the measurement area. This may also be the reason for the insufficient performance of the CSELT model, which is based on an over-roof-top Deygout multiple diffraction approach. The CSELT model has been proofed to perform better for higher mounted BS.

The performance of the tested models are summarised in Tab. 4.5.2, where the mean prediction errors and the corresponding standard deviations are given. An average standard deviation of the prediction error of about 7 dB up to 9 dB is achieved by the presented models, with exception of the TLM and ray tracing models of the Swiss Telecom PTT and the CSELT model, in which only 2D-horizontal contributions are taken into account.

It has to be noted that no vegetation effects are considered by any model. An interesting simulation result is that over-roof-top propagation and around-building propagation are fairly in the same order of magnitude. Differences between measurement and simulation may be due to the inaccuracies of the building data base, and of course due to the fact of disregarding further details of the real environment like cars, lamp posts, roof kind, balconies etc. However, the achieved results are very promising for both empirical-based as well as fully deterministic propagation models.

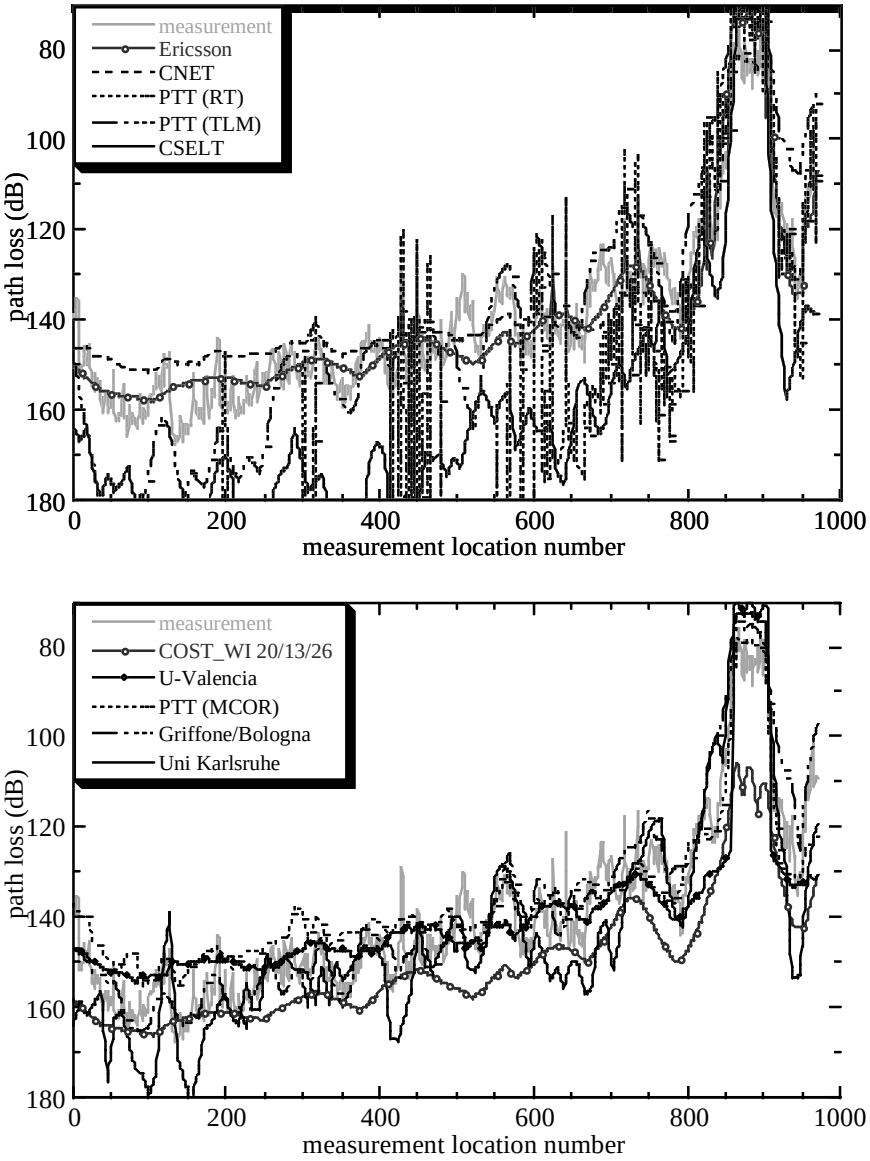

Fig. 4.5.3 Comparison between measured and predicted path loss along route METRO200 (see Fig. 4.5.2); ht = 13 m.

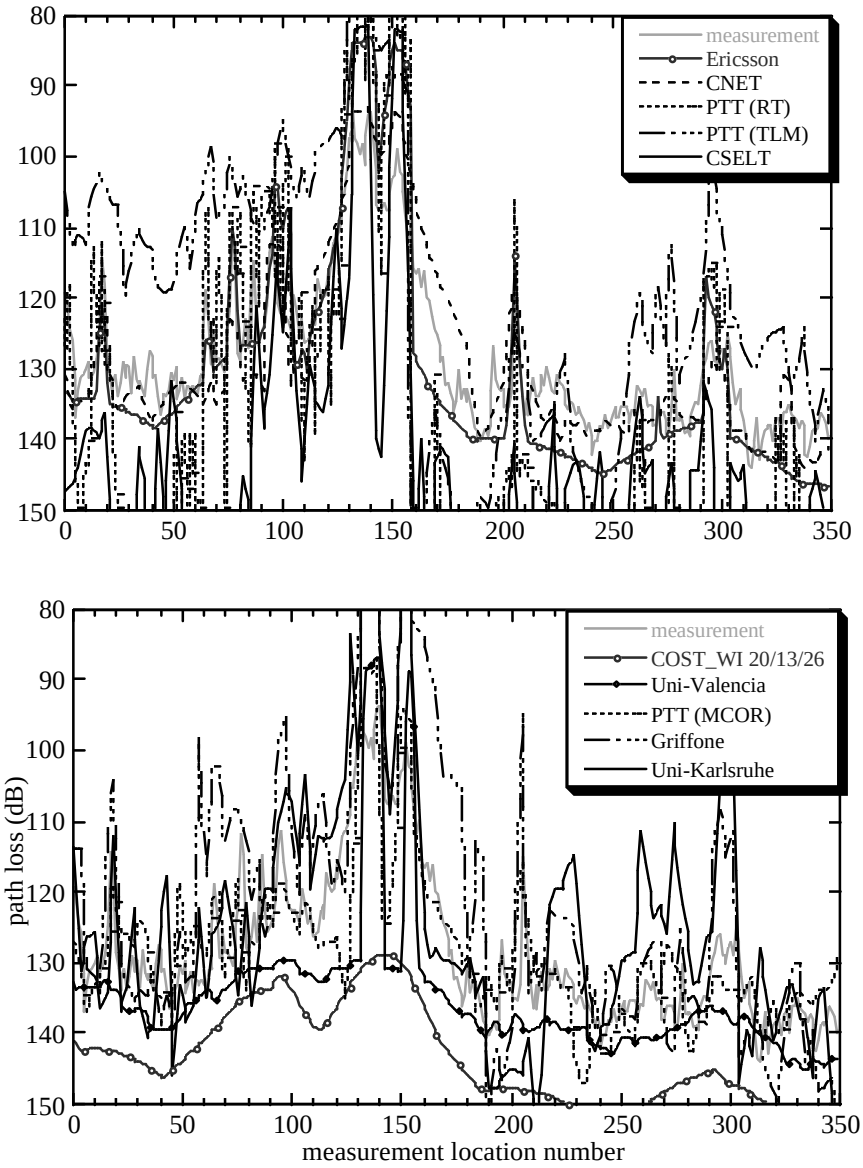

Fig. 4.5.4 Comparison between measured and predicted path loss along route METRO201 (see Fig. 4.5.2); ht = 13 m.

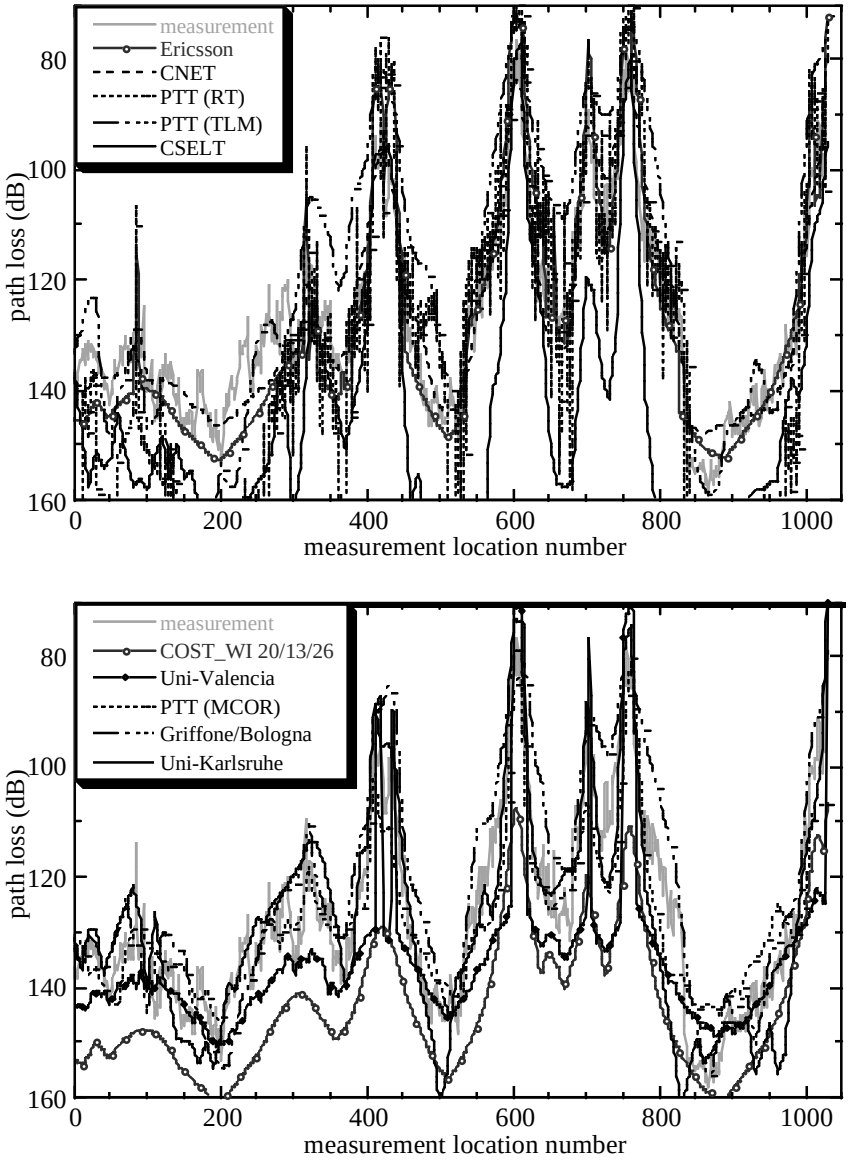

Fig. 4.5.5 Comparison between measured and predicted path loss along route METRO202 (see Fig. 4.5.2); ht = 13 m.

Prediction model	METRO200 (970 points)		METRO201 (355 points)		METRO202 (1031 points)		average
	STD (dB)	mean (dB)	STD (dB)	mean (dB)	STD (dB)	mean (dB)	**STD (dB)**
Ericsson	6.7	0.3	7.1	2.3	7.5	1.4	**7.1**
CNET	6.9	-2.1	9.5	-3.6	5.6	-0.2	**7.3**
PTT (RT)	14.6 [1)]	-6.1 [1)]	15.5 [2)]	-6.7 [2)]	12.3 [3)]	-1.1 [3)]	**14.1**
PTT (TLM)	13.8	0.8	21.7	6.7	12.9	6.5	**16.1**
COST-WI [4)]	7.7	10.8	5.9	15.4	7.3	16.3	**7.0**
Uni.-Valencia [5)]	8.7	0.2	7.0	-6.6	10.3	-7.4	**8.7**
CSELT	10.4	21.8	12.3	16.1	13.3	20.6	**12.0**
PTT (MCOR)	7.0	-3.3	6.2	-0.1	7.6	-1.1	**6.9**
Villa Griffone Lab	6.3	-1.7	10.9	-6.3	6.8	-5.5	**8.0**
Uni.-Karlsruhe	8.5 [6)]	-4.3 [6)]	9.1	2.4	8.6 [6)]	-1.0 [6)]	**8.7**

[1)]calculations at 425 points only; [2)]calculations at 264 points only; [3)]calculations at 774 points only; [4)]assumed terrain parameters: building height: 20m, street width: 13m, building separation: 26m; [5)]no 3D effects are considered; [6)]2D-vertical propagation plane only;

Tab. 4.5.2 Performance of the propagation models at 947 MHz; standard deviation and mean value (prediction - measurement).

4.6 Building Penetration

Jan-Erik Berg , Ericsson Radio Systems AB, Sweden

4.6.1 Introduction and definitions

A common approach in many existing planning tools is to predict the path loss outside in the proximity of the buildings and then add a constant loss in order to estimate the loss inside the building. This is a major reason why the building penetration loss usually is related to the outside levels at about 2 m height above ground.

Some concern must be taken when the median outside level is determined. If a line of sight exists between the exterior base station antenna and one or several external walls a considerable variation, tens of dB, of the path loss around the perimeter of the building may occur. Thus, the corresponding penetration loss will vary considerably depending on which reference level is used. The outside reference level must not contain both line of sight and non line of sight results!

The indoor small scale fading in an area of about 1 to 2 square metres is, for a narrowband signal in the frequency range 900-1800 MHz, usually close to a Rayleigh distribution (when the envelope variation is described in Volt). The large scale variation is obtained when this small scale fading component is removed by spatial filtering.

The penetration loss can be divided into four major categories:

- wall loss,
- room loss,
- floor loss,
- building loss,

each relative the median path loss level outside the building.

The wall loss, which is angle dependent, is the penetration loss through the wall. The true wall loss is difficult to determine when measurements are taken in a building due to multiple reflections and the furniture close to the walls.

For line of sight conditions with one dominant ray, the power of the reflected ray at the external wall can be considerable at small grazing angles, giving rise to a large penetration loss compared to perpendicular penetration.

The penetration loss of the external wall can be different at non line of sight conditions compared to a perpendicular line of sight situation. Thus, one single external wall can have considerable different penetration losses, depending on the environmental conditions.

The room loss is the median loss determined from measurements taken in the whole room about 1-2 m above the floor. In a room with an external wall, the room loss is usually greater than the corresponding external wall loss. The room loss level is practical to use when the penetration loss is displayed on a drawing describing the building. Sometimes is it practical to divide large rooms into smaller fictitious rooms.

Usually the measured room loss values are used as an input to a model which considers one or several propagating rays through the building. The difference between the model and measurements can be minimised by choosing appropriate losses for the different walls. This approach gives wall losses that can be used in the model but do not necessary represent the actual physical wall losses. The results in this chapter are mainly based on this method.

The floor loss is the median loss in all of the rooms on the same floor in a building. The large scale variation over the floor is often log-normal distributed. The building loss is similar to the floor loss, but taken over all of the floors in the building. When this method is used, information should be given if the basement is included or not.

In some cases the penetration loss decreases with increasing floor level. This dependence is called floor height gain and given in dB/floor. Due to that the heights of the storeys vary between different buildings, it is sometimes better to describe the dependence as a function of the physical height in dB/m. The height gain effect ceases to be applicable at floor levels that are considerable above the average height of the neighbouring buildings. The sum of the outside reference loss and the height gain loss, which is negative, must not be less than the free space propagation loss.

In micro-cellular environments, where the base station antenna height is considerable lower than the surrounding building height, the penetration loss for line of sight conditions is quite independent of the floor height at larger distances. This is also valid for non line of sight conditions when the main part of the power propagates along the streets. However, in non line of sight conditions where the dominant part of the received power in the street originates from rays that due to reflections and diffraction have propagated down from the surrounding roof level, a notable floor or height gain can be

found. This is usually the case in macro-cellular environments with a base station antenna height above the height of the average building height in the area.

Median is used in the definitions above, which is preferable due to its independence of the distribution. However, the main part of result presented below, are based on averaging.

4.6.2 Building penetration loss at line of sight conditions

Building penetration related papers written by COST 231 participants can be found in [120]-[134]. Results from a lot of different kind of buildings with miscellaneous distances and angles between the outdoor antennas and the surfaces of the external walls have been presented within the COST 231 project [120], [121], [123], [125], [128], [129], [131]-[134]. Different models have been proposed, each applicable for the actual measurement condition. With an attempt to describe all of the different propagation conditions in one single model, the approach described below is suggested. The parameters in the model are defined in Fig. 4.6.1.

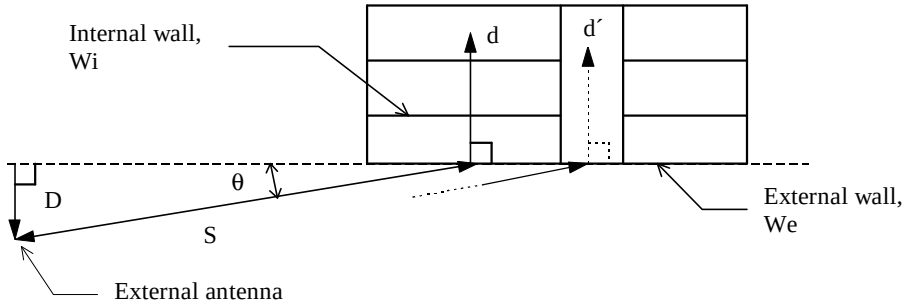

Fig. 4.6.1 Definition of grazing angle θ and distances D, S and d. In the building an example of a possible wall layout at one single floor is shown. The distance d is a path through internal walls and the distance d´ is a path through a corridor without internal walls.

The total path loss between isotropic antennas is determined with the following expression:

$$L\,/\,\mathrm{dB} = 32.4 + 20\log(f) + 20\log(S + d) + W_e + WG_e \cdot \left(1 - \frac{D}{S}\right)^2 + \max(\Gamma_1, \Gamma_2) \qquad (4.6.1)$$

$$\Gamma_1 = W_i \cdot p \tag{4.6.2}$$

$$\Gamma_2 = \alpha \cdot (d-2) \cdot \left(1 - \frac{D}{S}\right)^2 \tag{4.6.3}$$

D and d are the perpendicular distances and S is the physical distance between the external antenna and the external wall at the actual floor. All distances are in metres, frequency is in GHz. The angle is determined through the expression $\sin(\theta) = D/S$ [134]. The only case when $\theta = 90$ degrees is when the external antenna is located at the same height as the actual floor height and at perpendicular distance from the external wall, i.e. when D = S. Hence, θ changes considerably with floor height at short distances D. W_e is the loss in dB in the externally illuminated wall at perpendicular penetration $\theta = 90$ degrees. WG_e is the additional loss in dB in the external wall when $\theta = 0$ degrees. W_i is the loss in the internal walls in dB and p is the number of penetrated internal walls (p = 0, 1, 2...). In the case that there are no internal walls, as along d´ shown in Fig. 4.6.1, the existing additional loss is determined with a in dB/m. It should be noted that Γ_1 can be replaced with β d, with β in dB/m, if the average indoor wall loss W_i and the average distance between the indoor walls are known.

The suggested model assumes free space propagation path loss between the external antenna and the illuminated wall and is not based on an outdoor reference level. This approach has been found to be valid also for line of sight conditions at small angles θ in street micro-cells even when the path loss has been larger than free space propagation close to the surface outside the external wall. It has also been found that the model seems to generate an appropriate total loss in a street micro-cell environment, with buildings at both sides of the street, for the case when the external wall is obstructed from true line of sight conditions due to slightly shadowing neighbouring buildings [133]. In street micro-cells with buildings on both sides of the street, it could be appropriate not to use the actual distance D if it is very small. Due to reflections at the walls on the opposite side of the street, a larger value might be more suitable, e.g. half the width of the street. The model is based on measurements in the frequency range from 900-1800 MHz and at distances up to 500 m. The floor height dependence at short distances is based on very few measurements and the validity of the model for this case is vague. At short distances it might be appropriate to apply the indoor propagation models. It should be noted that the model fits the general behaviour of the path loss variation at different conditions quite well when many buildings are considered, however, there can be considerable

deviations for some explicit buildings. The following parameter values are recommended in the model:

W_e : 4 - 10 dB, (concrete with normal window size 7 dB, wood 4 dB)

W_i : 4 - 10 dB, (concrete walls 7 dB, wood and plaster 4 dB)

WG_e: about 20 dB

α : about 0.6 dB/m

The wall loss is not necessarily the physical loss for a single homogeneous wall, it is the loss that gives reasonable agreement when the model is applied and it includes objects in the building, such as cupboards, shelves and other furniture. Thin wood or plaster walls can give rise to lower losses than 4 dB and concrete walls without windows 10-20 dB. Increasing window sizes decreases the loss and vice versa. Metallized window-glass or metal reinforced glass can give rise to losses considerable greater than 10 dB. An absolute value is difficult to give, due to that one must also consider the size of the window and the amount of power that penetrates through the wall around the window. A combination of metal covered walls and metallized window-glass can give rise to quite high loss levels.

Typical floor losses, 900-1800 MHz, for buildings along a street with small grazing angles θ in an urban environment at distances S greater than 150 m is in the range of 27-37 dB and the large scale variation at one single floor is usually close to a log-normal distribution with a standard deviation from about 5-10 dB. At short distances, the floor loss can vary considerably, especially when it is related to the loss in the street at about 2 m height. This behaviour corresponds with the characteristic of the model which will give rise to a considerable variation due to its angle and distance dependence, θ and d. Typical floor losses, 900-1800 MHz, at one single floor level vary in the range of about 4-37 dB with a standard deviation of the large scale variation, at one single floor level, of 5-15 dB. For this case, strong deviations from the log-normal distribution can occur quite often. It has been reported that the time dispersion in urban street micro-cells does only increase slightly in a building compared to the level in the street [132].

4.6.3 Penetration loss at non line of sight conditions

For the scenarios shown below, the penetration loss is related to the outside loss L_1 and L_2 in Fig. 4.6.2, and L_a and L_b in Fig. 4.6.3, at about 2 m height above the ground.

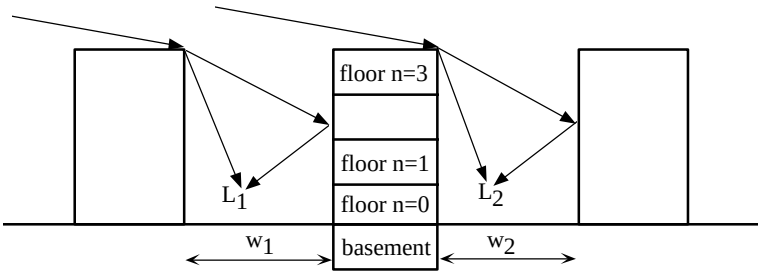

Fig. 4.6.2 Non line of sight scenario when the external antenna is located above the building height. The penetration loss is related to L_1 or L_2.

The floor height gain values given below are relevant when the width w_1, see Fig. 4.6.2, in the direction towards the external antenna is about 10-50 m. When w_1 increases, the floor height gain will decrease.

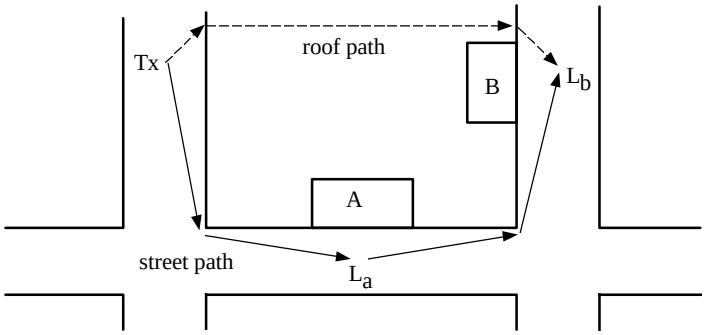

Fig. 4.6.3 Non line of sight scenario when the external antenna is located below the building height. The total area, except the streets, is assumed to be covered with buildings, though only building A and B are displayed. The penetration loss is related to L_a and L_b.

For the case when the penetration loss is related to L_2, the floor height gain will generally be less dependent of the width w_2. The total loss between isotropic antennas relative the outside reference loss, $L_{outside}$, is determined with the following equation [123], [124], [126], [130]-[132]:

$$L\ /\ \mathrm{dB} = L_{outside} + W_e + W_{ge} + \max(\Gamma_1, \Gamma_3) - G_{FH} \qquad (4.6.4)$$

$$\Gamma_3 = \alpha \cdot d \tag{4.6.5}$$

$$G_{FH} = \begin{cases} n \cdot G_n \\ h \cdot G_h \end{cases} \tag{4.6.6}$$

W_e, Γ_1, and d are similar to the corresponding definitions in the section above, line of sight conditions. The floor number is determined by n, see Fig. 4.6.2, and G_n is the floor height gain in dB/floor while G_h is the height gain in dB/m. h is the height in metres above the outdoor reference path loss level. Reported penetration losses of the external walls differ considerably, due to different measurement methods and, of course, due to different buildings. However, there might be a physical explanation of the noticed difference, which could justify the parameter Wg_e in the model, which is introduced in order to achieve unambiguous basic wall penetration losses.

The waves impinging on the external wall are distributed over a wide range of angles. Thus, by considering the angle dependent penetration loss, the loss will be larger compared to the case when one single wave, with equal power, penetrates perpendicularly through the wall. The difference should be more pronounced when one or several dominant waves are arriving at non perpendicular angles, which is most probable in this scenario. Another phenomenon, which could explain the increased penetration loss, is that the measured outside reference level is received from a combination of waves in the direction towards and waves reflected from the building, where the latter of course will not penetrate through the building. Similar condition is valid when perpendicular line of sight measurements are taken (with an omni antenna), but the relative power levels of the direct and the reflected wave will then be different and the direct wave will not suffer from extra angle dependent penetration loss. A value of about 3-5 dB is suggested for Wg_e at 900 MHz. In some measurements it has been found that the floor penetration loss increases 2 dB at 1800 MHz compared to 900 MHz, thus it is suggested that Wg_e(1800 MHz) = Wg_e(900 MHz) + 2 dB. The values on W_e and W_i given in the section above (LOS conditions) are recommended to be used. The a parameter has not been measured explicitly for this kind of scenario. Thus, at the moment, the value given in the section above (LOS conditions) is recommended, i.e. α = 0.6 dB/m. Reported values on G_n at 1800 MHz can be divided into two groups, in the range of 1.5-2 dB/floor and from 4-7 dB/floor. The latter values were taken from buildings with storey heights of about 4-5 m and it was found more appropriate to use the parameter G_h for these buildings, which varied from 1.1-1.6 dB/m at 1800 MHz. The floor height gain is lower at 900 MHz, but the difference is small. Floor

penetration loss at 1800 MHz has been found to vary between different buildings on the ground floor, n=0, from about 12-20 dB. The corresponding losses at 900 MHz were found to be about 2 dB lower. The large scale variation is log-normal, if there is no partial line of sight to the external wall, with a standard deviation of about 4-6 dB. No frequency dependence of the standard variation has been reported. The penetration loss into the basement, is about 20-30 dB, which can be either smaller or larger.

4.6.4 General building penetration model

It has been found that the best method in order to estimate the received power at a fixed location within a building, is to consider all the paths through the external walls as shown in Fig. 4.6.4 [131], [132]. For each path, the received power is determined according to the methods described above and the sum of these separate power levels will then be the total received power. Those paths that are expected to give rise to loss levels far greater than the remaining paths, can of course be omitted.

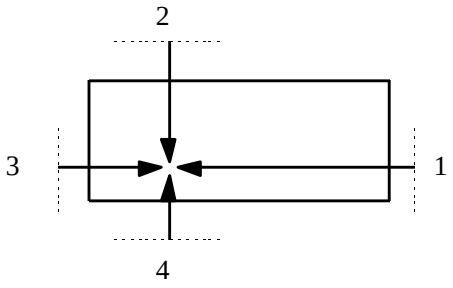

Fig. 4.6.4 Relevant propagation paths into a building.

The results in this chapter are based on measurements in the following towns and theoretical work performed by: Vienna, Technische Universität Wien (A), Aalborg, Aalborg University (DK), Turin, CSELT, (I), Madrid (E)/Telefónica Investigación y Desarollo, Stockholm (S)/Telia Research and Ericsson Radio Systems, Ipswich, Liverpool, London (UK) by British Telecom Research Laboratories, The University of Liverpool, and The University of Leeds.

4.7 Indoor Propagation Models

Jaakko Lähteenmäki , VTT Information Technology, Finland

4.7.1 General

Predicting the propagation characteristics between two antennas inside a building is important especially for the design of cordless telephones and WLANs (Wireless local area networks). Also the design of cellular systems with indoor base stations involves the use of indoor propagation models.

The indoor propagation channel differs considerably from the outdoor one. The distance between transmitter and receiver is shorter due to high attenuation caused by the internal walls and furniture and often also because of the lower transmitter power. The short distance implies shorter delay of echoes and consequently a lower delay spread. The temporal variations of the channel are slower compared to the conditions where the mobile antenna is mounted on a car. As is the case in outdoor systems, there are several important propagation parameters to be predicted. The path loss and the statistical characteristics of the received signal envelope are most important for coverage planning applications. The wide-band and time variation characteristics are essential for evaluation of the system performance by using either hardware or software simulation.

The considered propagation models are divided into four groups: empirical narrow-band models, empirical wide-band models, models for time variations and deterministic models. Empirical narrow-band models are expressed in a form of simple mathematical equations which give the path loss as the output. The equations are obtained by fitting the model to measurement results. Empirical wide-band models are expressed in a form of a table listing average delay spread values and typical power delay profile (PDP) shapes. Models for time variations are used for example to estimate the Doppler spectrum of the received signal. Deterministic models are calculation methods which physically simulate the propagation of radio waves. These models yield both narrow-band and wide-band information of the channel.

All of the presented models are based on propagation measurements. The measurement techniques and analysis are described in Sec. 2.2 and Sec. 2.3. Propagation measurements have mostly been carried out at 1800 MHz which

is most appropriate considering the future indoor systems. Scaling of results to other frequency bands will be discussed.

4.7.2 Empirical narrow-band models

Three types of empirical indoor models have been investigated.

The ***one-slope model*** *(1SM)* assumes a linear dependence between the path loss (dB) and the logarithmic distance

$$L = L_0 + 10n \cdot \log(d) \tag{4.7.1}$$

where

L_0 = the path loss at 1 meter distance,

n = power decay index,

d = distance between transmitter and receiver in metres.

This model is easy to use, because only the distance between transmitter and receiver appears as an input parameter. However, the dependency of these parameters on environment category (Tab. 2.3.1) has to be taken into account.

The multi-wall model [135]-[139] gives the path loss as the free space loss added with losses introduced by the walls and floors penetrated by the direct path between the transmitter and the receiver. It has been observed that the total floor loss is a non-linear function of the number of penetrated floors. This characteristic is taken into account by introducing an empirical factor b [139]. The ***multi-wall model*** *(MWM)* can then be expressed in form

$$L = L_{FS} + L_c + \sum_{i=1}^{I} k_{wi} L_{wi} + k_f^{\left[\frac{k_f+2}{k_f+1} - b\right]} L_f \tag{4.7.2}$$

where

L_{FS} = free space loss between transmitter and receiver,

L_{C} = constant loss,

k_{wi} = number of penetrated walls of type i,

k_f = number of penetrated floors,

L_{wi} = loss of wall type i

L_f = loss between adjacent floors,

b = empirical parameter,

I = number of wall types.

The constant loss in (4.7.2) is a term which results when wall losses are determined from measurement results by using the multiple linear regression. Normally it is close to zero. The third term in (4.7.2) expresses the total wall loss as a sum of the walls between transmitter and receiver. For practical reasons the number of different wall types must be kept low. Otherwise, the difference between the wall types is small and their significance in the model becomes unclear. A division into two wall types according to Tab. 4.7.1 is proposed.

It is important to notice that the loss factors in (4.7.2) are not physical wall losses but model coefficients which are optimised along with the measured path loss data. Consequently, the loss factors implicitly include the effect of furniture as well as the effect of signal paths guided through corridors.

Wall type	Description
Light wall (L_{w1})	A wall that is not bearing load: e.g. plasterboard, particle board or thin (<10 cm), light concrete wall.
Heavy wall (L_{w2})	A load-bearing wall or other thick (>10 cm) wall, made of e.g. concrete or brick.

Tab. 4.7.1 Wall types for the multi-wall model.

The third considered propagation model is the ***linear attenuation model (LAM)***, which assumes that the excess path loss (dB) is linearly dependent on the distance (m), where α (dB/m) is the attenuation coefficient:

$$L = L_{FS} + \alpha d \tag{4.7.3}$$

In some studies wall loss terms are added to the linear model which improves the performance to some extent since degrees of freedom is increased [140]. In the following the LAM is used in the simple form of (4.7.3).

Optimised model coefficients

The measurements listed in Table 2.3.2 have been used to optimise model coefficients for the three empirical models presented in the previous section.

The overall results calculated as an average of the available results from each environment category are listed in Table 4.7.2.

The multi-wall model coefficients have been optimised for the measurement category "dense". However, it can also be used in the other environments where the number of walls is small and multi-wall model yields results close to free space values.

The results given in Tab. 4.7.2. are relevant to buildings having normal type of furniture. In UPC the effect of furniture was studied. A decrease from 3.8 to 3.4 in the decay exponent was observed.

Environment	One slope model (1SM)		Multi-wall model (MWM)				Linear model (LAM)
	L_0 [dB]	n	L_{w1} [dB]	L_{w2} [dB]	L_f [dB]	b	a
Dense one floor two floors multi floor	33.3 [3)] 21.9 [4)] 44.9 [4)]	4.0 [3)] 5.2 [4)] 5.4 [4)]	3.4 [1)]	6.9 [1)]	18.3 [2)]	0.46 [9)]	0.62 [10)] 2.8 [4)]
Open	42.7 [5)]	1.9 [5)]	3.4 [1)]	6.9 [1)]	18.3 [2)]	0.46 [9)]	0.22 [8)]
Large	37.5 [6)]	2.0 [6)]	3.4 [1)]	6.9 [1)]	18.3 [2)]	0.46 [9)]	
Corridor	39.2 [7)]	1.4 [7)]	3.4 [1)]	6.9 [1)]	18.3 [2)]	0.46 [9)]	

[1)]Alcatel, CNET, TUW, UPC, VTT; [2)]Alcatel, CNET, UPC, VTT; [3)]UPC, TUW; [4)]VTT; [5)]TUW; [6)]VTT, UPC; [7)]Alcatel; [8)]Lund; [9)]VTT, Ericsson; [10)]TUW, Lund

Tab. 4.7.2 Results for model coefficients for path loss models at 1800 MHz. The expressions „one floor“, „two floors“ and „multi floor“ mean that Tx and Rx have been within the same floor, within two adjacent floors or within more than two floors.

Frequency dependency

Measurements in 5 buildings ([141], [142]) at both 900 MHz and 1800 MHz bands have been conducted. In these measurements the separation of receiver and transmitter is up to 5 floors. According to the results the path loss difference between the frequency bands is typically slightly higher than would be predicted in free space. Considering the Multi-wall model, a difference of 1.5 dB in the light wall loss and a difference of 3.5 dB in the floor loss were reported. This is in line with the results of Ericsson, which report 2.1 dB loss for plasterboard wall at 900 MHz [139]. Considering the One slope model, L_0 should be reduced by 10 dB [141] in the multi floor

case. In the single floor case the appropriate reduction is 7-8 dB. For the decay index, n, same value may be applied both at 900 MHz and at 1800 MHz.

Fading

The empirical propagation models presented above yield the mean path loss at a given location. In practical application of the models it is important to know also the statistics of the received signal. Two fading mechanisms can be identified: long term fading and short term fading.

In indoor environments the long term fading is understood as fluctuations of the mean value calculated over a distance of a few wavelengths. According to measurements in Lund and UPC the indoor long term fading follows log-normal distribution with σ = 2.7-5.3 dB. Short fading has been observed to follow Rice and Rayleigh distributions. The K-value varies from negative values (Rayleigh distribution) in NLOS conditions up to 14.8 dB in clear LOS conditions.

Temporal short term fading is understood as fast fluctuations of the signal level caused by movements in the propagation environment. In environments with low level of movements or LOS condition the temporal fading has been observed to follow the Rice distribution with K=7-14 dB. In an environment with NLOS condition and a lot of movements in the environment, the temporal fading follows the Rayleigh distribution [143]. In [144] the Weibull and Nakagami distributions have been found best in describing the temporal variability.

4.7.3. Empirical wide-band models

Empirical wide-band model is considered as a means for evaluation of the delay spread and average power delay profile (PDP). One of these two factors together with Doppler characteristics (see Sec. 2.1) are typically required as an input to system simulations. The overall results (i.e. results averaged over an environment category) of wide-band measurements are listed in Table 4.7.3. As expected, the delay spread has lowest values in dense environment and larger values in open and large environments. The dependency of the delay spread on the dimensions of the environment can even be utilised in prediction as shown in [136], [140], [145].

Environment	Average rms delay spread [ns]	Variability of rms delay spread [ns]	Typical profile shape
Dense: Lund	22.5	5-40 [1)]	power/exponential
VTT	15.3	3.4 [2)]	exponential
TUW	20.0	8-31 [3)]	-
Average	**19.3**		
Open: Lund	35.0	5-95 [1)]	power
VTT	17.7	3.1 [2)]	power
ETH	30.5	4.1 [2)]	exponential
Average	**27.7**		
Large: VTT	55.4	27.2 [2)]	exponential
ETH	79.4	4.3 [2)]	exponential
Average	**67.4**		

[1)]Peak-to-peak of instantaneous delay spread, [2)]Standard deviation of delay spread local averages, [3)]Peak-to-peak of delay spread local averages

Tab. 4.7.3 Delay spread and PDP shape in different environments.

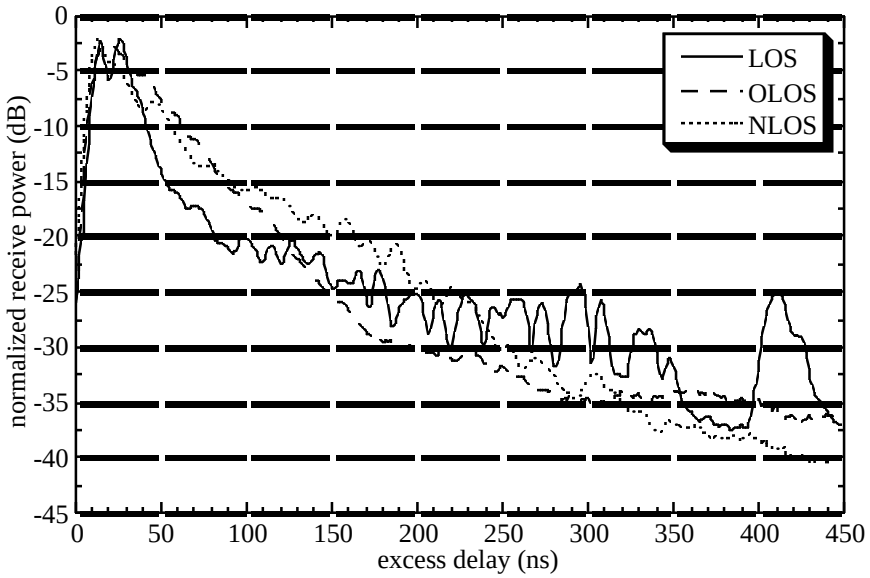

Fig. 4.7.1 Overall average power delay profiles in three configurations (Lund).

Although instantaneous values and local averages of the PDP may include a lot of environment dependent details, the overall average PDP has quite regular shape. As seen in Table 4.7.3, the PDP in dense environment has been observed to follow either power function (the decay is logarithmic in

dB scale) or exponent function (the decay is linear in dB scale). In open environment the PDP follows best the power function, because of the strong effect of the direct path. Typical averaged power delay profiles in Line-of-sight (LOS), Non-line-of-sight (NLOS) and Obstructed-line-of-sight (OLOS) conditions are shown in Fig. 4.7.1. OLOS means a condition where the direct path is blocked only by one obstacle, e.g. a piece of furniture.

4.7.4 Modelling the time fluctuations of the indoor channel

Bernard Fleury, Aalborg University, Denmark

Time variations of the indoor radio channel essentially result from the following three mechanisms: As the location of the receiving antenna changes, the spatial fluctuations of the electric field along the receiver trajectory are translated into corresponding time variations. Time variability also arises when the orientation of the antenna changes, due to its usually non-isotropic field pattern. Finally, movements of scattering objects such as persons or furniture also contribute to make the channel system functions time-variant. Time-variations of the mobile channel have been studied earlier e.g., in [146]-[148]. Almost all attention has focused on the time-variability resulting from receiver movements with constant velocity. However, the consideration of such receiver displacements in the indoor environment is questionable since they are not realistic for describing human motion. Moreover, they force to restrict the investigations of the spatial field dependency to one specific direction determined by the receiver velocity vector. Finally, such movements do not allow to take the Doppler rate, i.e., the change of Doppler frequency, into account.

A stochastic model is proposed which reproduces a succession of realistic typical human movements performed in a random manner [149]. The model derivation relies on deterministic models which have been empirically derived from free arm movements (see references reported in [149]). The receiver trajectory is modelled as:

$$\bar{x}(t) = g(t / T) * \left[\sum_{i=1}^{\infty} \Delta\bar{x}_i \delta(t - t_i) \right] \tag{4.7.4}$$

where

$\{t_i\}$ is an homogeneous Poisson process with expected occurrence rate L,

2. $\{\Delta\dot{x}_i\}$ is a sequence of independent random vectors with zero mean and covariance matrix ςI_3, with I_3 being the 3-dimensional identity matrix,
3. the two sequences $\{t_i\}$ and $\{\Delta\dot{x}_i\}$ are independent.

The random 3-dimensional step process within the brackets describes the succession of new or corrective actions. It is convoluted with an appropriately time-scaled unit stroke function g(t) which models the smoothing due to body inertia. Under the usual assumptions on the phase of the incident waves, the time-variant channel resulting from receiver displacements according to (4.7.4) is WSSUS over the time interval [T, ∞) with a scattering function of the form:

$$P(\tau,\nu) = P(\tau)\cdot P_n(\nu) \tag{4.7.5}$$

where P(t) and P_N(n) are the power delay profile and the normalised power Doppler profile, respectively, of the channel. The normalised time correlation function of the channel, which is the inverse Fourier transform of P_N(n) has been derived in [149].

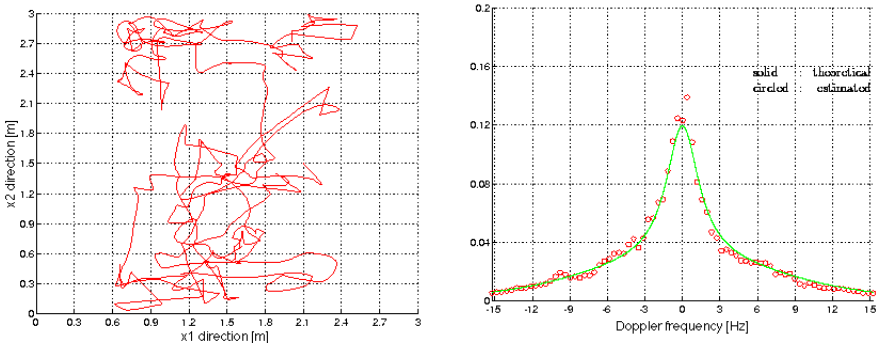

Fig. 4.7.2: a) Simulated receiver trajectory b) Estimated and theoretical normalised power Doppler profile.

A realisation of the first two components of $\dot{x}(t)$ is depicted in Fig. 4.7.2.a. The normalised power Doppler profile has been estimated in a real environment where the receiving antenna performs random movements according to (4.7.4) with the above setting. In Fig. 4.7.2.b, the estimate of P_N(n) is compared with the curve theoretically derived from the model. For

the simulation, the parameter values and the unit stroke have been selected as follows [149]:

$$g(t)=\begin{cases} 0 & ; \quad t<0 \\ -t^3\left(15t-6t^2-10\right) & ; \quad 0\le t\le 1 \\ 1 & ; \quad t>0 \end{cases} \tag{4.7.6}$$

T=220 ms, ς=10 cm, Λ = 10 s^{-1}

4.7.5. Deterministic models

Jaakko Lähtenmäki, VTT Information Technology Finland
Dieter J. Cichon, IBP Pietzsch, Germany

Deterministic models are used to simulate physically the propagation of radio waves. Therefore the effect of the environment on the propagation parameters can be taken into account more accurately than in empirical models. Another advantage is that deterministic models make it possible to predict several propagation parameters. For example, the path loss, impulse response and angle-of-arrival can be predicted at the same time.

Several deterministic techniques for propagation modelling can be identified. For indoor applications, especially, the Finite Difference Time Domain (FDTD) technique and the geometrical optics (GO) technique have been studied. In COST 231 the main effort is on the geometrical optics which is more computer efficient than the FDTD. There are two basic approaches in the geometrical optics technique. The ray launching approach and the image approach. Computational complexity of ray-tracing methods is considered in [150].

Ray launching model (RLM)

The ray launching approach involves a number of rays launched at the transmit antenna in specified directions. For each ray its intersection with a wall is determined and the incident ray is divided into a wall penetrating ray and a reflected ray; each of them is traced to its next intersection and so on. A ray is terminated when its amplitude falls below a specified threshold, or a chosen maximum number of ray-wall interactions are succeeded. In, e.g., [151] a uniform angular separation of launching rays is maintained, where the spherical surface is subdivided by a geodesic polyhedron with resulting hexagonally shaped, wavefront portions, which are further approximated by

circular areas. Whether a ray reaches a receiver point or not can be accomplished by a reception sphere [152].

In Fig. 4.7.3 a two-dimensional view of the reception sphere is shown, where the unfolded total path length d and the angular separation γ of adjacent rays launched at Tx determine its radius R_{rs}:

$$R_{rs} = \gamma\, d / \sqrt{3} \tag{4.7.7}$$

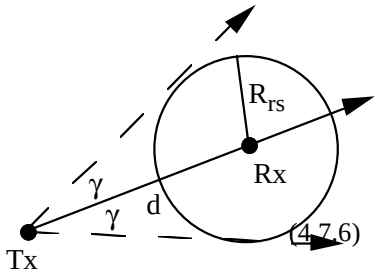

(4.7.6)

Fig. 4.7.3 2D view of the reception sphere.

However this is an approximate solution for the 3D propagation case. To achieve a complete solid angle discretisation under maintenance of unambiguous and practical reception determination, the entire solid angle 4π is subdivided into rectangularly shaped, incremental portions of the spherical wavefront [153], [154]. In [102], [154] the propagation directions ϑ_i and ψ_i of the central rays of the ray tubes and the corresponding ray tube angles $\Delta\vartheta_i$ and $\Delta\psi_i$ as depicted in Fig. 4.7.4 are determined by (4.7.8) and (4.7.9).

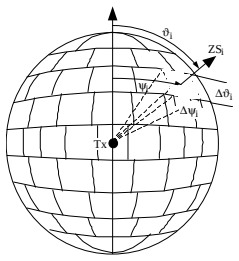

Fig. 4.7.4 Ray launching.

$$\Delta\psi_i(\vartheta_i) = \frac{\Delta\vartheta}{\sin\vartheta_i} \tag{4.7.8}$$

$$\vartheta_i = \frac{\Delta\vartheta}{2} + (i-1)\Delta\vartheta\,, \quad i = 1\ldots N_\vartheta\,, \quad \Delta\vartheta = \text{const.} \tag{4.7.9}$$

Ray launching approaches are flexible, because diffracted and scattered rays can also be handled along with the specular reflections,. To maintain a sufficient resolution the so called "ray splitting technique" can be used as given in [153] and [103].

Image approach method (IAM)

The image approach [112], [155] makes use of the images of the transmit antenna location relative to all the surfaces of the environment. The coordinates of all the images is calculated and then rays are traced towards these images. First and second order reflections can be calculated very fast

without sending rays to all directions. The disadvantage is that calculation time grows exponentially when the order of calculated reflections is increased. Therefore the image approach is suitable for semi-deterministic modelling, where the main signal paths, i.e. direct path and most important specularly reflected and diffracted rays are calculated in a deterministic way while more complicated phenomena are taken into account by using empirical factors. The effect of bookshelves and cupboards covering considerable parts of walls is taken into account by including an additional loss to the wall penetration loss. An additional loss of 3 dB was observed to be appropriate. This additional loss is introduced in context of walls covered by bookshelves, cupboards or other large pieces of furniture. Furthermore, it was found necessary to set an empirical limit for the wall transmission loss which otherwise becomes very high when the angle of incidence is large. The wall transmission loss is limited to twice the value (in dB) for normal incidence.

Material	Uni-Karlsruhe (ray launching)		VTT (image approach)		Typical thickness
	ε_r'	ε_r''	ε_r'	ε_r''	
concrete	9	0.9	6	0.7	25 cm
light concrete	-	-	2	0.5	10 cm
brick	-	-	4	0.1	13 cm
plasterboard	6	0.6	2.5	0.1	2 x 1.3 cm
particle board	-	-	3	0.2	2 x 1.3 cm
wood	2.5	0.03	-	-	5 cm
glass	6	0.05	6	0.05	2 x 0.3 cm
bookshelf	2.5	0.3	-	-	30 cm

Tab. 4.7.4 Material parameters [156]-[158]

Building information

Deterministic models require detailed building information, i.e. location and material parameters of walls, floors and even furniture. Usually, accurate information of materials and internal structures of walls and floors is not available and somewhat approximate values have to be adopted. The used material parameters are listed in Tab. 4.7.4. Also the typical thickness for an internal wall of each material is given.

4.7.6 Comparison of the performance of the path loss models

Jaakko Lähtenmäki, VTT Information Technology Finland
Dieter J. Cichon, IBP Pietzsch, Germany

The performance of the propagation models was tested against three data sets. The data sets are labelled according to the organisation who has performed the measurements: Alcatel, TUW and VTT. Each building under test has normal office furniture. In one building (VTT) the base station (BS) is in different floor than most of the mobile stations. In the other buildings BS and the mobile stations are in the same floor.

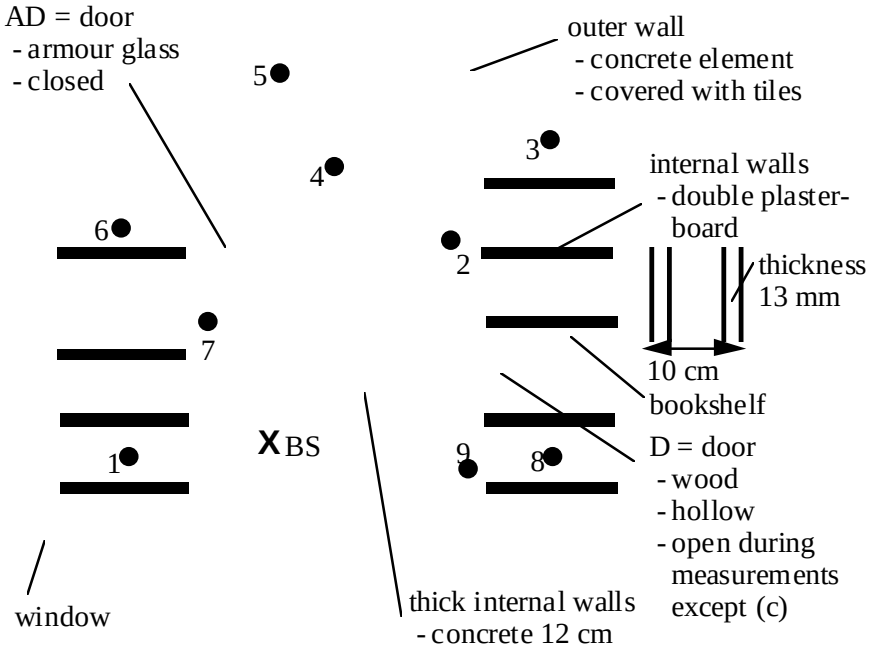

Fig. 4.7.5 Map of the 2nd floor of the office building (data set: VTT) with marked base and mobile locations (1-9).

The Alcatel data set is measured in an indoor environment with a typical office architecture: Large office rooms are located along a main corridor. Internal walls are made of thin wood panel and they are classified as "light walls". The environment category is "open" and it includes 56 measurement points. There are two base station locations: transmitter in the corridor and transmitter in one of the working rooms.

The TUW data set is measured in a "dense" indoor environment consisting of mostly small office rooms along a corridor. The walls are made of concrete and brick and they are classified as "heavy". The data set includes 40 measurement points.

The VTT data set is measured in a 7-floor building. The material of the internal walls of the working rooms is plasterboard ("light walls"). The walls in the centre of the building are concrete/light concrete ("heavy"). The data set belongs to category "dense" and it includes 9 measurement points within the same floor with the base station, which is in the second floor, and 45 measurement points are distributed in floors 3-7. For the testing of the RLM model, only the data from floors 2-5 have been used. The floor plan of the second floor is shown in Fig. 4.7.5. Other floors are essentially similar. Considering the propagation between floors, it is important to note that a similar building is located at 80 metre distance and another building having 2 floors is located at 15 metre distance.

Table 4.7.5 lists means and standard deviations (STD) of the prediction errors of the 5 models in case of single-floor propagation. The ray-launching model (RLM) takes into account up to 5 reflections and 12 transmissions per ray; the image model (IAM) is also a three-dimensional model and takes into account first and second order reflection as well as 3 most important diffraction points. The diffraction is calculated by using the Uniform Geometrical Theory of Diffraction (UTD). The empirical one-slope model and linear model are included for reference. Mean prediction errors and standard deviations in case of multi-floor propagation for mobile locations in the 3rd-4th floor and in the 3rd-5th floor, respectively, are given in Tab. 4.7.6.

	1SM		**MWM**		**LAM**		**IAM**		**RLM**	
data set / frequency	STD (dB)	mean (dB)	STD (dB)	mean (dB)	STD (dB)	mean (dB)	STD (dB)	mean (dB)	STD (dB)	mean (dB)
Alcatel, O: 1900 MHz	5.7	-1.6	4.2	2.2	4.7	-0.8	4.3	-0.4	-	-
TUW, D: 1800 MHz	10.0	-0.7	9.5	-10.3	7.8	-7.5	7.0	-3.8	-	-
VTT, D; 2nd floor only:										
856 MHz	8.6	19.2	4.4	-4.5	8.5	4.7	6.0	-11.7	4.2	3.3
1800 MHz	7.5	20.6	2.0	-2.7	8.4	6.5	4.1	-2.8	8.9	3.3

Tab. 4.7.5 Performance of the models for single floor propagation (mean error: predicted - measured path loss)

When analysing the results, it has to be noted that the three empirical models (using the coefficients given in Tab. 4.7.2) are compared to the measurement data without any fitting or adjustment. For the IAM, the furniture loss and the limit for the penetration loss were introduced after the first comparisons with the measurement data.

	1SM		**MWM**		**LAM**		**IAM**		**RLM**	
data set: VTT, D	STD (dB)	mean (dB)	STD (dB)	mean (dB)	STD (dB)	mean (dB)	STD (dB)	mean (dB)	STD (dB)	mean (dB)
3rd-4th floor:										
856 MHz	10.3	-2.7	8.3	-8.2	10.2	-16.1	9.0	-2.7	6.2	0.3
1800 MHz	12.2	-7.3	7.1	-11.1	11.6	-20.3	11.3	10.3	8.7	0.1
3rd-5th floor:										
856 MHz	10.7	-7.1	7.9	-7.2	9.7	-19.6	7.8	-2.6	9.1	-4.6
1800 MHz	11.9	-11.8	7.5	-9.7	10.9	-23.8	10.9	11.7	11.8	-5.7
3rd-7th floor:										
856 MHz	9.6	-10.6	9.4	-5.0	8.6	-19.5	8.4	-3.7	-	-
1800 MHz	10.0	-14.1	10.2	-5.9	9.8	-22.7	13.5	7.3	-	-

Tab. 4.7.6 Performance of the models for multi-floor propagation (mean error: predicted - measured path loss).

From the empirical models the Multi-wall model (MWM) gives best results although the difference to One slope model (1SM) is small. The MWM has a large mean error in TUW building where the heavy walls seem to be more lossy than in other buildings. The TUW building is relatively old (older part is built in 1910 and newer part is built in 1932) and the wall structures are thick especially between the old and new part of the building. All of the models perform well in the Alcatel building which is open and has a low number of walls. The advantage of the MWM and the deterministic models (IAM and RLM) is most clearly seen in the case when the transmitter and receiver are in different floors (VTT). The LAM yields worst results in average. One reason for this may be that the used values for attenuation coefficient are based on a small data set: Many COST 231 documents give model coefficients only for the MWM and the 1SM. Calculated and measured path loss values of the VTT data set in an office building are compared at a frequency of 856 MHz and 1800 MHz in Fig. 4.7.6 and Fig. 4.7.7, respectively. The mobile station is in the 2nd floor (points: 1-9), in the 3 rd floor (points: 10-18), in the 4th floor (points: 19-27) and in the 5th floor (points: 28-36). The general trend is that prediction accuracy is better when the vertical separation between transmitter and receiver is low. The performance of the 1SM and LAM is poor because they only take into account the distance and not the number of penetrated floors.

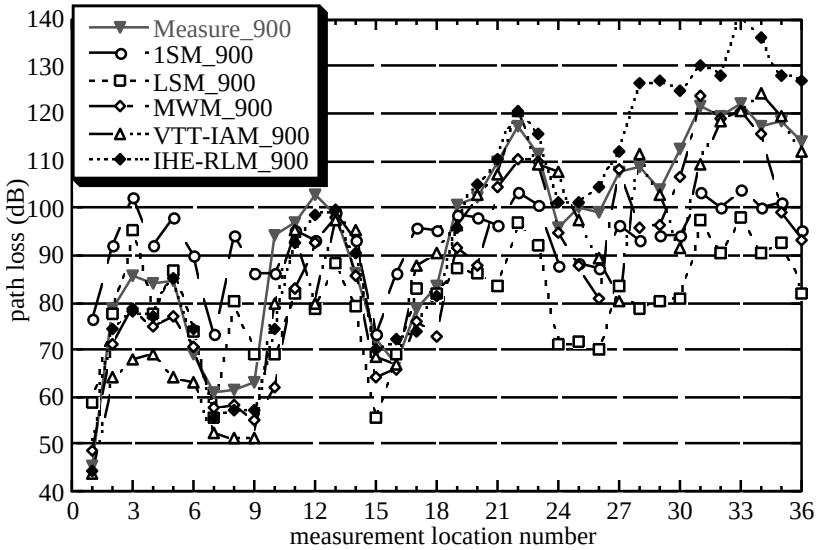

Fig. 4.7.6 Performance of empirical and ray optical propagation models at 856 MHz in 4 successive floors (base station in the 2nd floor; see Fig. 4.7.5).

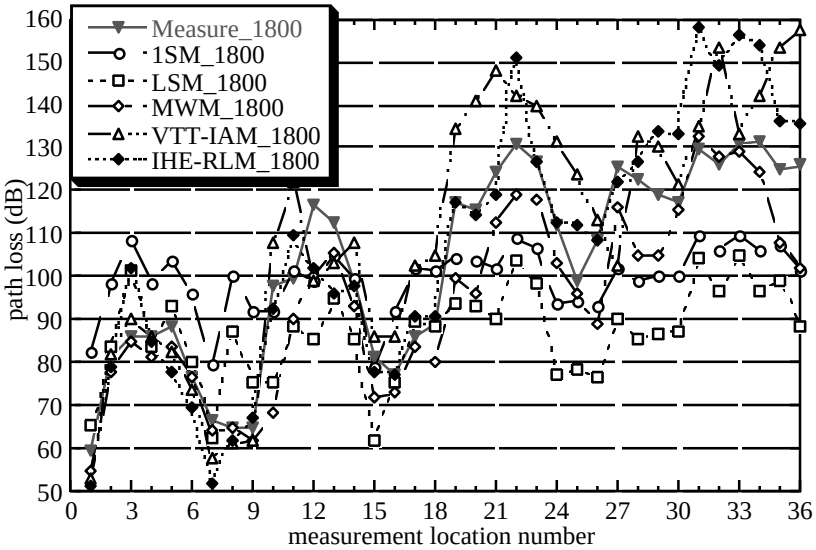

Fig. 4.7.7 Performance of empirical and ray optical propagation models at 1800 MHz in 4 successive floors (base station in the 2nd floor; see Fig. 4.7.5).

4.8 Tunnels, Corridors, and other Special Environments

Ernst Bonek , Technical University of Vienna, Austria

4.8.1 Tunnels

Wave propagation in tunnels shows different effects than in other environments due to guidance by the walls, at least at frequencies higher than 800 MHz. Even very rough tunnels driven into plain rock show good waveguiding when no installations are present [159]. The power loss observed is, in most cases, less than free space attenuation. There is a waveguiding gain, so to speak. Thus it is appropriate to consider the tunnel as an overmoded waveguide with lossy dielectric walls.

Power loss decreases with increasing frequency which is proven for frequencies up to 17 GHz by simulations and measurements, showing a slightly increasing slope of power loss up to 60 GHz [159]-[161]. Simulations of the GSM-SDCCH channel found the tunnel environment to be the least demanding case among rural or urban situations, and the lowest transmitter power is needed for a minimum E_b/N_0 [162].

In tunnels, the distinction between short-term and large-scale fading is not as usual. In a smooth and straight tunnel short-term fading transforms into long and flat fades due to small phase differences between the individually reflected paths. Only close to the source short term effects caused by higher order mode excitation are observed. The source may be either an antenna inside the tunnel, the entrance aperture, or leaky feeder cables, or any secondary source, like vehicles or installations [163], [164]. If the source is distributed (leaky cable), short term fading occurs along the entire tunnel, of course. In contrast, feeding the tunnel by internal or external discrete antennas, there are usually only a small number of paths with about the same power incident at a given position. In general, heavier short term fading effects appear at higher frequencies despite the lower average loss, since the effective roughness of tunnel walls is wavelength dependent.

The small phase difference of individual paths with only few wall reflections tends to reduce the delay spread of the signal as it propagates further down the tunnel. (Paths with many reflections are subject to repeated reflection loss and die out fast.) This delay spread reduction by tunnel propagation has been experimentally proven [165]. It should be noted that corridors in buildings behave, very much like (short) tunnels, as waveguides.

Experimental proof has been given in [140] and [17]. The measured decrease in delay spread, after an expected initial rise, versus transmitter-receiver separation in a corridor is shown in Fig. 4.8.1. Multiple reflections caused by corridor ends have been measured and identified up to 8^{th} order.

4.8.2 Loss models and coverage

Different empirical models are proposed to describe propagation in tunnels as well as along corridors.

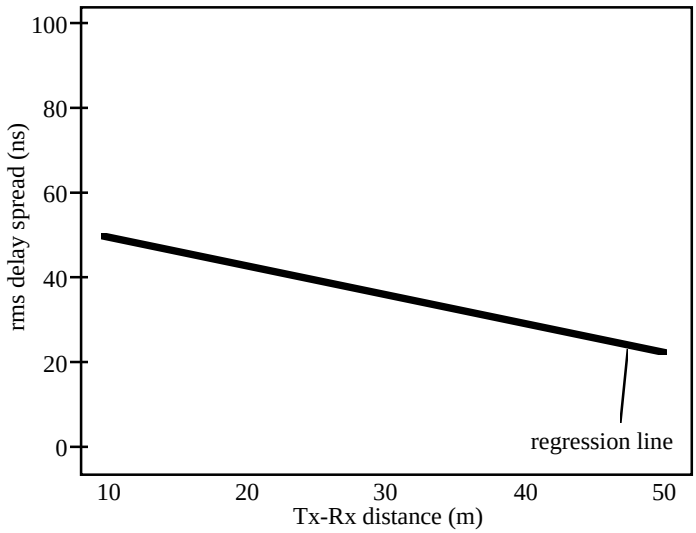

Fig. 4.8.1 Delay spread in a corridor versus Tx-Rx separation.

Commonly used are the standard model using parameter fitting (one-slope, two-slope), the waveguide model giving an attenuation in dB per unit length and the combination of both models (see also Sec. 4.7.2). Confined spaces with well-reflecting walls allow application of ray tracing approaches (see also Sec. 4.7.5). Some major effects in tunnels can be described using just a small number of rays, sometimes as few as two. As an example of the usefulness of ray tracing for tunnels, Fig. 4.8.2 compares a measurement run in a rather rough, irregularly shaped tunnel with a ray tracing simulation based on the simplifying assumption of rectangular cross section.

A slightly different point-of-view re-arranges all reflections into an array of image antennas [166]. This description leads to the hypothesis that all reference distances of propagation in tunnels or corridors should be given as multiples of the Rayleigh distance, called "critical distance", l_{crit},

$$l_{crit} = \frac{D^2}{\lambda} \tag{4.8.1}$$

where D is the largest cross dimension of the waveguiding structure and λ is the free-space wavelength. At such a distance the phase differences between individual paths become smaller than a certain value (e.g. $\lambda/2$). Coverage in road tunnels can be predicted by the following equation,

$$P_r = P_0 - l \cdot \alpha_0 \tag{4.8.2}$$

where P_r is the received power level in dB at a length l away from the antenna (down the tunnel), P_0 is the reference level measured at l_0 away from the antenna, and α_0 is the tunnel and frequency specific loss factor [165].

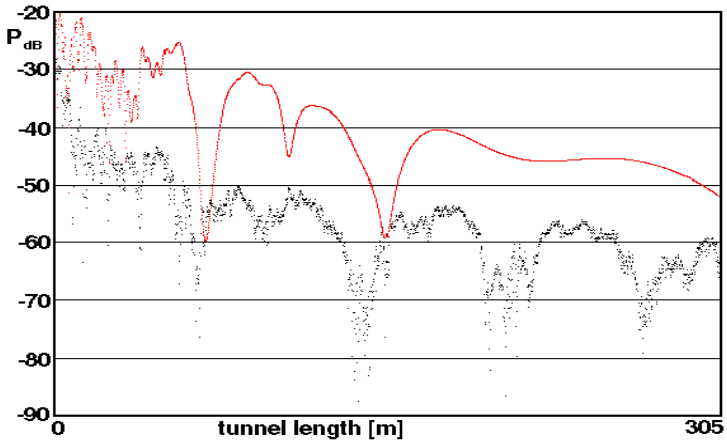

Fig. 4.8.2 Signal strength in a naturally rough tunnel at 960 MHz as compared to ray tracing (20 dB shifted).

Two reference measurements are needed to determine P_0 and α_0 for a given type of tunnel. Averaging should be done over a length of about $l_{crit}/10$, which is large to smooth out fades, but small enough not to avoid waveguide attenuation effects. For a practical calculation of propagation loss or coverage distance l_{cov}, a probability margin (e.g. level difference between 50% and 99% coverage probability, M_{99}) has to be included to get [165]

$$l_{cov} = l_{crit} + (P_0 - M_{99} - P_{min}) / \alpha_0 \tag{4.8.3}$$

where P_{min} is the system specific minimum received power.

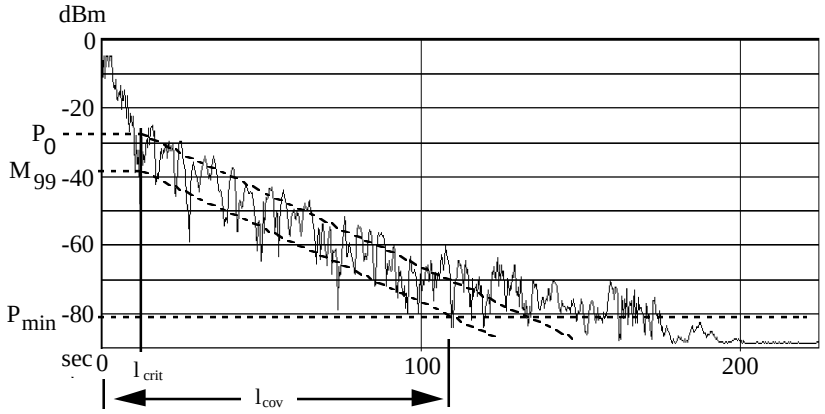

Fig. 4.8.3 Measured signal level in road tunnel and fitted model (f = 960 MHz, v = 80 km/h, 100 sec = 1.9 km)

Situation	P_0 [dBm]	C [dB]	a_0 [dB/km]	M_{95} [dB]	M_{99} [dB]	l_{cov}.(95/99%) [km]
960 MHz, 53dBm ERP, Tx in niche	-25	78	20	8	13	3.3 / 3 (both directions)
960 MHz, 53dBm ERP, Tx 67m outside	-23	76	18-22	8	13	~3.3 / 3
1800 MHz, 46dBm ERP, Tx in niche	-45	91	14	12	18	3 / 2.7 (both directions)
1800 MHz, 46dBm ERP, Tx 67m outside	-48	94	15	12	18	2.7 / 2.4
1800 MHz, 46dBm ERP, Tx 67m outside northern entrance	-55	101	20 (15)	12	18	1.7 / 1.4

Tab. 4.8.1 Observed power levels and coverage lengths in a Euro-standard two-lane road tunnel.

Fig. 4.8.3 shows a sample measurement and the fitted model and Table 4.8.1 gives numbers for several situations of these measurements [165].

One implicit assumption for the use of (4.8.3) is the independence of coupling loss into the tunnel and propagation loss inside the tunnel. The validity of this assumption was also proven by experiment in [165].

Interesting enough, traffic does add fades but only a few dB additional loss, if enough space over or between vehicles is left for wave propagation. Such is the case in Euro-standard road tunnels and in tunnels for high speed trains. Tunnel bends with curvature radii commonly used in such tunnels do not significantly hamper wave propagation, even if the bend is 90 degree.

4.8.3 Leaky feeders

The classic solution of tunnel communication, leaky feeders, is now also available for 900 MHz. Cables designed for 900 MHz even show acceptable performance at 1800 MHz with, of course, a general decrease of received power level [167]. Compared to natural propagation leaky cables increase delay spread, but with less pronounced short-term-fading effects. Hence the Rice-parameter is lower than when using discrete antennas in the tunnel. Special cables have been manufactured that compensate for the longitudinal cable loss and the radiating loss. Mean signal level remains fairly constant over several hundred meters. Fig. 4.8.4 shows the field strength distribution along the tunnel achieved with a longitudinally compensated leaky feeder [168]. Combinations of leaky feeders terminating in a directive antenna have been shown to smoothen out signal variations and to extend coverage, but a beating phenomena between cable and antenna signals may occur. A still further alternative are so-called mode converters [168], i.e. coaxial cables with repeated radiating sections.

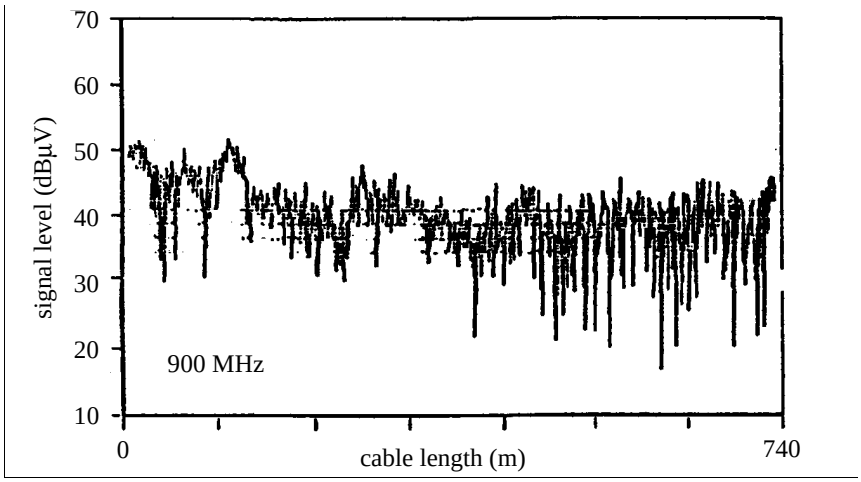

Fig. 4.8.4 Signal level in tunnel with compensated leaky feeder cable.

Between them the signal is guided as usual inside the ordinary coaxial cable.

Other approaches studied for serving GSM in confined areas by the DRIVE project ICAR include the booster concept which retransmits radio signals from the BTS to the MS and vice versa (Fig. 4.8.5). This concept is not directly tied to leaky cables and can be applied with directive antennas as well.

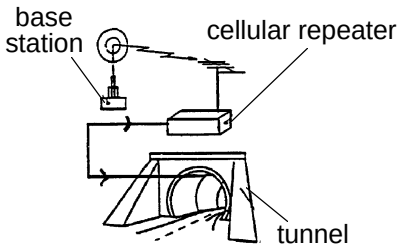

Fig. 4.8.5 Booster concept to cover confined areas.

4.8.4 Railway environment and high-speed trains

The cuttings along modern railway lines can guide electromagnetic waves in quite a similar way as tunnels or street corridors. The low base station antenna and the rather high mobile antenna in addition to guiding structures like overtop wires, are responsible for flat fading effects. In general, low delay spread can be observed and Doppler spectra degenerate to a few, often a single, distinct peaks, i.e. Doppler spread is very small [169]. This has been observed as well in road tunnels with smoothly flowing traffic at constant speed [170]. An appropriate fading statistic is Ricean in connection with a rather high Rice parameter [169]. The railway environment is a favourable case for line coverage (as opposed to area coverage in ordinary mobile communications) [169], [171]. The predetermined neighbouring cell facilitates handover, and no unexpected turns will occur. A measurement campaign on high-speed trains in France and Germany [172] revealed the annoying fact that the usual tinted windows introduce an extra loss of 25-30 dB. Non-metallized, transparent windows do not cause significant added loss, unless wave incidence is grazing.

Another interesting finding was that field strength coverage alone may not be sufficient for GSM operation, because mobiles have problems in synchronising and decoding control messages at speeds around and above 250 km/h. This, however, could be a problem of the specific mobile station used. Fig. 4.8.6 shows the speed profile of the TGV Nord for a journey from Lille to Paris, the synchronisation information (number of detected neighbouring cells), and the signal strength reported by the mobile. Still, GSM is capable of meeting the requirements for radio communications for many applications foreseen for high-speed trains going up to 200 km/h [173].

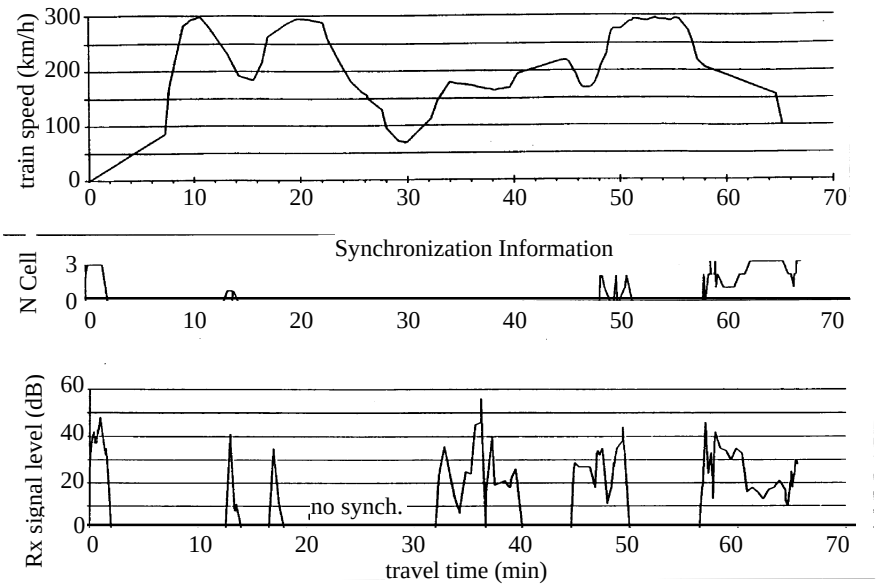

Fig. 4.8.6 Speed profile, synchronisation information and signal level along high-speed train line "TGV Lille-Paris".

Antennas mounted on the driver´s cab roof bypass the mentioned problem of metallized window attenuation. For passengers using handportables either repeaters [173] - which will have to meet extremely tough dynamic-range problems - or completely novel concepts with a "moving base station" [171] have been proposed.

4.8.5 Scaled-model measurements

Model-scaled measurements are a proper tool for investigations of propagation in or around tunnels, cuttings, and some indoor environments. For frequencies in the range of 2nd and 3rd generation cellular networks, scaling factors of at least 10 call for measurements above 10 GHz. Scaled measurements allow to separate individual influence parameters on wave propagation, like cross-section shape, entrance environment, antenna mounting, vehicles, and additional traffic. Many observed propagation effects are in line with measured data in real-size tunnels [164]. This pertains, e.g., for propagation differences in different lanes and the deep fade mitigation by traffic or other obstacles in the tunnel.

4.9 References

[1] S. W. Marcus, "A hybrid method for computing transmission losses in an inhomogeneous atmosphere over irregular terrain," *IEEE Trans. on Antennas and Propagation*, vol. 40, no. 12, Dec. 1992, pp. 451-1458

[2] D. T. Moroney, "Computational methods for the calculation of electromagnetic scattering from large scale perfect electrical conductors," Ph.D. Thesis, The University of Dublin Trinity College, 1995

[3] R. H. Hardin, F. D.Tappert, "Application of the split step Fourier method to the numerical solution of non-linear and variable coefficient wave equations," SIAM Rev. 15(1973), p. 423

[4] D. J. Cichon, (in German) "Strahlenoptische Modellierung der Wellenausbreitung in urbanen Mikro- und Pikofunkzellen," ("Ray optical modelling of wave propagation in urban micro- and pico-cells"), Ph.D. Thesis, University of Karlsruhe, published in *Forschungsberichte aus dem Institut für Höchstfrequenztechnik und Elektronik der Universität Karlsruhe***,** vol. 8, ISSN 0942-2935, 1994

[5] D. J. Cichon, T. C. Becker, M. Döttling, "Ray optical prediction of outdoor and indoor coverage in urban macro- and micro-cells," *Proc. IEEE Vehicular Technology Conference VTC'96*, Atlanta, USA, April 18-May 1, 1996, pp. 41-45

[6] D. McGirl, P. C. Fannin, "Digital Elevation Modelling," *COST 231 TD(94)75*, Prague, Czech Republic, 1994

[7] J. Lähteenmäki,, "Testing and verification of indoor propagation models," *COST 231 TD(94)111*, Sept 1994

[8] E. Lachat, J.-F. Wagen, J. Li, "Effect of building heights on predictions in munich using multiple vertical knife-edge propagation," *COST 231 TD(96)24*, Jan 1996

[9] B. E. Gschwendtner, "Practical investigation using ray optical prediction techniques in microcells," *COST 231 TD(94)127*, 1994

[10] D. Grace et al., "The effects of building position tolerances on ray based urban propagation modelling," *COST 231 TD(95)16*, January 1995

[11] R. Petersilka, "E-plus, an integrated approach using GIS in mobile communications," SMALLWORLD International Conference, Robinson College, Cambridge, October 1995

[12] M. Perucca, B. Gschwendtner, "Aspects of ray-optical modelling in microcells," *COST 231 TD(95)82*, Florence, Italy, April 1995

[13] A. Glassner (editor), *An Introduction to Ray Tracing*, Academic Press, San Diego, 1989

[14] RACE 2084, "Definition of a data format for wide-band propagation measurements and explanation of how to use the data," *COST 231 TD(94)025*, 1994

[15] H. Bühler, T. Klemenschits, "UMF The Universal Measurement File-Format," *COST 231 TD(93)26*, Barcelona, Spain, January 1993

[16] U. Dersch, E. Zollinger, "Physical characteristics of urban micro-cellular propagation," *IEEE Trans. on Antennas and Propagation*, vol. 42, no. 11, pp. 1528-1539, Nov. 1994

[17] U. Dersch, J. Troger, E. Zollinger, "Multiple reflections of radio waves in a corridor," *IEEE Trans. on Antennas and Propagation*, vol. 42, no. 11, Nov. 1994, pp. 1571-1574

[18] A. J. Levy, " Fine structures of the urban mobile propagation channel," *Proc. COMMSPHERE´91,* December 1991, pp. 5.1.1-5.1.6

[19] J.-P. Rossi, A. J. Levy, "A ray model for decimetric radiowave propagation in an urban area," *Radio Science*, vol. 27, no. 6, pp. 971-979, Nov.-Dec. 1992

[20] J.-F. Wagen, K. Rizk, "Ray tracing based prediction of impulse response in urban microcells," *44th IEEE Vehicular Technology Conference (VTC'94)*, pp. 210-214 , June 1994

[21] B. Chopard, P. Luthi, J.-F. Wagen, "Wave propagation in urban microcells: A massively parallel approach using the TLM method," *COST 231 TD(95) 33*, Bern, Switzerland, January 1995

[22] F. Lotse, J.-E. Berg, R. Bownds, "Indoor propagation measurements at 900 MHz," *IEEE Vehicular Technology Conf. VTC'92*, pp. 629-632, May 1992

[23] J.-E. Berg, J. Ruprecht, J.-P. de Weck, A. Mattsson, "Specular reflections from high-rise buildings in 900 MHz cellular systems," *41st IEEE Vehicular Technology Conference VTC'91,* pp. 594-599 , May 1991

[24] J. Walfisch, H. L. Bertoni, "A theoretical model of UHF propagation in urban environments," *IEEE Trans. on Antennas and Propagation*, vol. 36, no. 12, pp. 1788-1796, Dec. 1988

[25] J. H. Causebrook, "Vodafone's fieldstrength prediction method," *COST 231 TD(93)1*, Barcelona, Spain, 1993

[26] P. Kreuzgruber, T. Bründl, W. Kuran, R. Gahleitner, "Prediction of indoor radio propagation with the ray splitting model including edge diffraction and rough surfaces," *COST-231 TD(94) 50*, Prague, Czech Republic, April 1994

[27] R. Jakoby, U. Liebenow, "Modelling of radiowave propagation in microcells," Proc. *Intern. Conference on Antennas and Propagation ICAP´95*, Eindhoven, The Netherlands, pp. 377-380

[28] L. B. Felsen, N. Marcuvitz, *Radiation and Scattering of Waves,* Prentice-Hall Inc., Englewood Cliffs, New Jersey, Sec. 6.4 and 6.5, 1973

[29] J.-F. Wagen, M. Keer, "Comparison of diffraction coefficients for propagation prediction in microcells," *COST-231 TD(93) 80*, Grimstad, Norway, May 1993

[30] J. B. Keller, " Geometrical Theory of Diffraction," *J. Opt. Soc. Am.*, vol. 52, pp. 116-130, 1962

[31] D. A. McNamara, C. W. I. Pistorius, J. A. G. Malherbe, *Introduction to the Uniform Geometrical Theory of Diffraction*, Artech House, Norwood, MA, USA, 1990, ISBN 0-89006-301-X

[32] C. Bergljung, "Diffraction of Electromagnetic Waves by Dielectric Wedges," Ph.D. Thesis, Lund Institute of Technology, Sweden, 1994

[33] M. Keer, (in French) "La Representation Spectrale de la Diffraction dans le Domaine Spatial," ("Spectral representation of diffraction in spatial domain"),

Ph.D. Thesis No 1069, Swiss Federal Institute of Technology, Switzerland, 1992

[34] R. J. Luebbers, "A heuristic UTD slope diffraction coefficient for rough lossy wedges," *IEEE Trans. on Antennas and Propagation*, vol. 37, no. 2, pp. 206-211, 1989

[35] J.-F. Sante, "Measurements and modelling in rural areas," *COST-231 TD(93) 121*, Limerick, Ireland, September 1993

[36] P. Möller, "Urban area radio propagation measurements and comparison to a new semi-deterministic model," Diplomarbeit, Universidad Politécnica de Valencia and Universität Karlsruhe, Spain and Germany, 1994

[37] S. Guérin, (in French) "Modélisation physique de la propagation des ondes radioélectriques en milieu urbain," ("Physical modelling of radio wave propagation in urban area"), Rapport de stage, Institut Galilée Télé-communications et CNET, 1992

[38] J.-F. Wagen, "SIP simulation of UHF propagation in urban microcells," *41st IEEE Vehicular Technology Conference VTC'91*, St. Louis, USA, May 1991

[39] S. R. Saunders, F. R. Bonar, "Explicit multiple building attenuation function for mobile radio wave propagation," *Electronics Letters*, vol. 27, no. 14, pp. 1276-1277, July 1991

[40] J. B. Andersen, "Transition zone diffraction by multiple edges," *IEE Proc. Microwaves, Antennas and Propagation*, vol. 141, no. 5, October 1994, pp. 382-384

[41] J. B. Andersen, J.Wiart, "UTD transition zone diffraction," *COST 231 TD(96)3*, Belfort, January 1996

[42] L. Vogler, "An attenuation function for multiple knife edge diffraction," *Radio Science*, 17, 1982, pp. 1541-1546

[43] ITU Recommendation ITU-R 526-2, 1994 PN Series Volume "Propagation in non-ionized media," pp. 129-149, 1994

[44] J. Li, J.-F. Wagen, E. Lachat, "On the ITU model for multi-knife edge diffraction", submitted to IEE, also in *COST 231 TD(96)25*, Belfort, January 1996; *paper available from: Dr. J-F. Wagen, Swiss Telecom PTT, Mobile Communications, FE 421, CH-3000 Bern 29, Switzerland*

[45] L. R. Maciel, H. L. Bertoni, H. H. Xia, "Unified approach to prediction of propagation over buildings for all ranges of base station antenna height," *IEEE Trans. on Vehicular Technology* , vol. 43, no. 1, 1993, pp. 35-41

[46] P. Beckmann, A. Spizzichino, *The Scattering of Electromagnetic Waves from Rough Surfaces*, MacMillan, New York, 1963

[47] K. Rizk, J.-F. Wagen, S. Bokhari, F. Gardiol, "Comparison between the diffraction theory and the moment method for the scattering by surface irregularities in a building wall," *Journées Internationales de Nice sur les Antennes (JINA'94)*, Nice, France, Nov. 1994

[48] F. Ikegami, S. Yoshida, M. Umehira, "Propagation factors controlling mean field strength on urban streets," *IEEE Trans. on Antennas and Propagation*, vol. 32, no. 8, August 1984, pp. 822-829

[49] M. Hata, "Empirical formula for propagation loss in land mobile radio services," *IEEE Trans. on Vehicular Technology*, vol. 29, pp. 317-325, 1980

[50] Y. Okumura, E. Ohmori, T. Kawano, K. Fukuda, "Field strength and its variability in VHF and UHF land-mobile service," *Review of the Electrical Communication Laboratory*, vol. 16, no. 9-10, 1968, pp. 825-873

[51] COST 231, "Urban transmission loss models for mobile radio in the 900- and 1,800 MHz bands (Revision 2)," *COST 231 TD(90)119 Rev. 2*, The Hague, The Netherlands, September 1991

[52] S. R. Saunders, F. R. Bonar, "Prediction of mobile radio wave propagation over buildings of irregular heights and spacings," *IEEE Trans. on Antennas and Propagation*, vol. 42, no. 2, pp. 137-144, 1994

[53] K. Löw, "Comparison of CW-measurements performed in Darmstadt with the flat edge model," *COST 231 TD(92)8*, Vienna, January 1992

[54] K. Löw, "Comparison of urban propagation models with CW-measurements," *Proc. Vehicular Technology Conference VTC´92*, pp. 936-942, 1992

[55] L. Ladell, "Transmission loss predictions in wooded terrain," *Proc. Nordic Radio Symposium NRS´86*, Sweden, 1986, pp. 41-50, ISBN 91-7056-072-2

[56] H. H. Xia, H. L. Bertoni, "Diffraction of cylindrical and plane waves by an array of absorbing half-screens," *IEEE Trans. on Antennas and Propagation*, vol. 40, no. 2, 1992, pp. 170-177

[57] L. R. Maciel, H. L. Bertoni, H. H. Xia, "Propagation over buildings for paths oblique to the street grid," *Proc. PIMRC´92*, Boston, USA, pp. 75-79

[58] Th. Kürner, (in German) "Ein modulares Konzept zur Feldstärkeprädiktion urbaner DCS-1800 Makrozellen," ("A modular concept for fieldstrength prediction of urban DCS 1800 macro cells"), *ITG-Fachbericht 135, Proceedings ITG-Fachtagung Mobile Kommunikation* , Neu-Ulm, September 1995, pp. 35-42

[59] Th. Kürner, R. Fauß, A. Wäsch, "A hybrid propagation modelling approach for DCS1800 macro cells," *Proc. IEEE VTC´96*, Atlanta, Georgia, USA, April 28-May 1, 1996, pp. 1628-1632

[60] N. Cardona, P. Möller, F. Alonso, " Applicability of Walfisch-type urban propagation models," *Electronics Letters*, vol. 31, no. 23, November 1995

[61] P. Eggers, "Note on the usage of Walfisch-type urban path loss prediction models," *COST 231 TD(91)87*, The Hague, September 1991

[62] R. Leppänen, J. Lähteenmäki, S. Tallqvist, "Radiowave propagation at 900 and 1800 MHz bands in wooded environments," *COST 231 TD(92)112*, Helsinki, 1992

[63] Th. Kürner, D. J. Cichon, W. Wiesbeck, " The influence of land usage on UHF wave propagation in the receiver near range," *IEEE Transactions on Vehicular Technology*,vol. 46, no. 3, August 1997, pp. 739-747

[64] T. Tamir, "Radio wave propagation along mixed paths in forest environments," *IEEE Trans. on Antennas and Propagation*, vol. 25, no. 4, 1977, pp. 471-477

[65] J. T. Hviid, J. B. Andersen, J. Toftgard, J. Bojer, "Terrain-based propagation model for rural areas - an integral equation approach," *IEEE Trans. on Antennas and Propagation*, vol. 43, no. 1, January 1995, pp. 41-46

[66] D. Moroney, P. J. Cullen, "A fast integral equation approach to UHF coverage estimation," *Proc. of the Joint COST 227/231 Workshop*, Florence/Italy, April 1995, published in *Mobile and Personal Commuincations*, edited by. E. del Re, Elsevier 1995, pp. 343-350

[67] J. E. Berg, H. Holmquist, "An FFT multiple half-screen diffraction model," *Proc. IEEE VTC'94*, Stockholm, Sweden, pp. 195-199, 1994

[68] J. E. Berg, "A macrocell model based on the parabolic differential equation," *Proc. Virginia Tech's Fourth Symposium on Wireless Personal Communications*, pp. 9.1-9.10, June 1-3, 1994

[69] M. Lebherz, W. Wiesbeck, W. Krank, "A versatile wave propagation model for the VHF/UHF range considering three dimensional terrain," *IEEE Trans. on Antennas and Propagation*, vol. 40, no. 10, October 1992, pp. 1121-1131

[70] P. Kuhlmann, "A forward-scattering algorithm for prediction of the direct-link in a three-dimensional model," *COST 231 TD(95)137*, Poznan, September 1995

[71] Th. Kürner, R. Fauß, (in German) "Untersuchungen zur Feldstärkeprädiktion im 1800 MHz-Bereich," ("Investigation of path loss algorithms at 1800 MHz"), Nachrichtentechnik Elektronik, ne-Science, vol. 45 (1995), no. 2, pp.18-23

[72] M. Badsberg, J. B. Andersen, P. Mogensen, "Exploitation of the terrain profile in the Hata model," *COST 231 TD(95)9*, Bern, January 1995

[73] K. E. Stocker, F. M. Landstorfer, "Empirical prediction of radiowave propagation by neural network simulator," *Electronics Letters*, vol. 28, no. 8, April 1992, pp. 724-726

[74] K. E. Stocker, B. E. Gschwendtner, F. M. Landstorfer, "An application of neural networks to prediction of terrestrial wave propagation for mobile radio," *IEE Proceedings-H*, vol. 140, no. 4, August 1993, pp. 315-320

[75] Th. Kürner, (in German) "Charakterisierung digitaler Funksysteme mit einem breitbandigen Wellenausbreitungsmodell," ("Characterisation of digital radio systems using a wideband propagation model"), Ph.D. Thesis, University of Karlsruhe, published in *Forschungsberichte aus dem Institut für Höchstfrequenztechnik und Elektronik*, vol. 3, ISSN 0942-2935, 1993

[76] G. A. Dechamps, "High frequency diffraction by wedges," *IEEE Trans. on Antennas and Propagation*, vol. 33, no. 4, April 1985, pp. 357-368

[77] P. Kuhlmann, (in German) "Schätzung der Funkfelddämpfung mit einem theoretischen Vorwärtsstreumodell," ("Path loss estimation using a theoretical forward scattering model"), *Proceedings Kleinheubacher Berichte 38*, 1995, pp. 175-184

[78] J. Bach Andersen, J. Hviid, J. Toftgard, "Comparison between different path loss prediction models," *COST 231 TD(93)6*, Barcelona, January 1993

[79] N. Geng, W. Wiesbeck, "Parabolic equation method simulations compared to measurements," *IEE International Conference on Antennas and Propagation ICAP´95*, Eindhoven, The Netherlands, April 1995, pp. 359-362

[80] D. Moroney, P. Cullen, " An integral equation approach to UHF coverage estimation," *IEE ICAP´95*, April 1995, pp. 367-372

[81] Th. Kürner, D.J. Cichon, W. Wiesbeck, "Concepts and results for 3D digital terrain based wave propagation models - an overview," *IEEE Journal on Selected Areas in Communications*, vol. 11, no. 7, pp. 1002-1012, 1993

[82] T. C. Becker, Th. Kürner, D. J. Cichon, "Fast scatterer search algorithms for 3D wave propagation modeling," *COST 231 TD(95)10*, Bern, 1995

[83] Th. Kürner, T. C. Becker, W. Wiesbeck, "Comparison of measured and predicted locations of interfering scatterers," *Proc. IEE ICAP´95*, Eindhoven, The Netherlands, April 1995, pp. 363-366

[84] H. Bühler, E. Bonek, B. Nemsic, "Estimation of heavy time dispersion for mobile radio channels using a path tracing concept," *Proc. IEEE VTC'93*, Secaucus, New Jersey, USA, pp. 257-260, 1993

[85] K. Davidsen, M. Danielsen, "Predicting impulse responses in mountainous areas," *Proc. PIMRC'94*, The Hague, The Netherlands, pp. 25-27

[86] P. Eggers, C. Jensen, A. Oprea, K. Davidsen, M. Danielsen, "Assessment of GSM-link quality dependence on radio dispersion in rural environments," *Proc. IEEE VTC'92*, Denver, May 1992, pp. 532-535

[87] U. Liebenow, P. Kuhlmann, "Theoretical investigations and wideband measurements on wave propagation in hilly terrain," *Proc. IEEE VTC'94*, Stockholm, Sweden, pp. 1803-1806

[88] U. Liebenow, (in German) "Ein dreidimensionales Ausbreitungsmodell im Vergleich mit Messungen," ("A three-dimensional propagation model compared to measurements"), *ITG-Fachbericht 135, Proc. ITG Mobile Kommunikation*, Neu-Ulm, 1995, pp. 43-50

[89] U. Liebenow, P. Kuhlmann, "A three-dimensional wave propagation model for macrocellular mobile communication networks in comparison with measurements," *Proc. IEEE VTC´96*, Atlanta, USA, April 28-May 1, 1996, pp. 1623-1627

[90] Th. Kürner, D. J. Cichon, W. Wiesbeck, "Evaluation and verification of the VHF/UHF propagation channel based on a 3D-wave propagation model," *IEEE Trans. on Antennas and Propagation*, vol. 44, no. 3, March 1996, pp. 393-404

[91] D. J. Cichon, T. Kürner, W. Wiesbeck, "Polarimetric aspects in antenna related superposition of multipath signals," *IEE Proc. Eighth Intern. Conf. on Antennas and Propagation ICAP'93*, pp. 80-83, Edinburgh, United Kingdom, March 30 - April 2, 1993

[92] J. H. Causebrook, "Signal attenuation by buildings and trees," *COST 231 TD(90)106*, Darmstadt, 1990

[93] J. Bach Andersen, "Issues and challenges of propagation studies for mobile networks," in *Proc. Personal, Indoor and Mobile Radio Conference PIMRC´94*, pp. 1285-1291, The Hague, The Netherlands, September 1994

[94] H. L. Bertoni, W. Honcharenko, L. R. Maciel, H. H. Xia, "UHF propagation prediction for wireless personal communications," *Proceedings of the IEEE*, vol. 82, no. 9, pp. 1333-1359, 1994

[95] U. Kauschke, "Propagation and system performance simulations for the short range DECT system in microcellular urban roads," *IEEE Trans. on Vehicular Technology*, vol. 44, no. 2, pp. 253-260, November 1994

[96] J. Wiart, P. Metton, "Terrain influence on line of sight microcellular propagation," *COST 231 TD(95)78*, Florence, Italy, April 1995

[97] H. Börjeson, C. Bergljung, P. Karlsson, L. O. Olsson, S.-O. Öhrvik, "Using a novel model for predicting propagation path loss," *COST 231 TD(93) 86*, Grimstad, Norway, May 1993

[98] H. Börjeson, C. Bergljung, L.G. Olsson, "Outdoor microcell measurements at 1700 MHz," *Proc. 41th IEEE Vehicular Technology Conference*, 1992

[99] J.-E. Berg, "A recursive method for street microcell path loss calculations," *6th PIMRC´95*, Toronto, Canada, September 1995, pp. 140-143

[100] J. Wiart, "Microcell modelling when base station is below roof tops," *Proc. 44th IEEE Vehicular Technology Conference VTC´94*, Stockholm, Sweden, May 25-28, 1994, pp. 200-204

[101] K. Rizk, J.-F. Wagen, F. Gardiol, "Ray tracing based path loss prediction in two microcellular environments," in Proc. *Personal, Indoor and Mobile Radio Conference PIMRC´94*, pp. 384-388, The Hague, The Netherlands, 18-23 September, 1994

[102] D. J. Cichon, T. C. Becker, W. Wiesbeck, "A ray launching approach for indoor and outdoor applications," *COST 231 TD(94)32*, Lisbon, Portugal, January 1994

[103] D. J. Cichon, W. Wiesbeck, "Indoor and outdoor propagation modeling in pico cells," in Proc. *Personal, Indoor and Mobile Radio Conference PIMRC´94*, pp. 491-495, The Hague, The Netherlands, September 1994

[104] D. J. Cichon, T. Kürner, W. Wiesbeck, (in German) "Modellierung der Wellenausbreitung in urbanem Gelände," ("Wave propagation modelling in urban area"), *FREQUENZ*, vol. 47, no. 1-2, pp. 2-11, 1993

[105] N. Cardona, F. Navarro, P. Möller, "Applicability of Walfisch-type urban propagation models," *COST 231 TD(94)134*, Darmstadt, Germany, September 1994

[106] P. Möller, N. Cardona, D. J. Cichon, "Investigations in a new developed urban propagation model," *COST 231 TD(94)135*, Darmstadt, Germany, September 1994

[107] J. Deygout, "Multiple knife-edge diffraction of microwaves," *IEEE Trans. on Antennas and Propagation*, vol. 14, no. 4, pp 480-489, 1966

[108] CCIR, vol. V Report 567-4, "Propagation data and prediction methods for the terrestrial land mobile service using the frequency range 30 MHz to 3 GHz"

[109] T. Kürner, D. J. Cichon: "Comments on TD (93) 6: Comparison between different path loss prediction models", *COST 231 TD(93)81*, Grimstad, Norway, May 1993

[110] M. Perucca, "Small cells characterization using 3-D database and Deygout diffraction approach," *COST 231 TD(94)54*, Prague, Czech Republic, April 1994

[111] J. P. Rossi, J. C. Bic, A. J. Lévy, "A ray launching model in urban area," *COST 231 TD(90)78,* Paris, France, October 1990
[112] U. Dersch, E. Zollinger, "Propagation mechanisms in microcell and indoor environments," *IEEE Trans. on Vehicular Technology*, vol. 43, no. 4, pp. 1058-1066, November 1994
[113] P. Daniele, V. Degli-Esposti, G. Falciasecca, G. Riva, "Field prediction tools for wireless communications in outdoor and indoor environments," *Proc. IEEE MTT-Symp. European Topical Congress "Technologies for Wireless Applications,"* Turin, Italy, November 1994
[114] A. Ishimaru, *Wave propagation and scattering in random media*, vols. I and II, Academic, New York, 1978
[115] B. E. Gschwendtner, (in German) "Adaptive Wellenausbreitungsmodelle für die Funknetzplanung," ("Adaptive propagation models for radio network planning"), Ph.D. Thesis, University of Stuttgart, ISBN 3-8265-1318-5, 1995
[116] B. E. Gschwendtner, G. Wölfle, B. Burk, F. M. Landstorfer, "Ray tracing vs. ray launching in 3-D microcell modelling," Proc. *European Personal and Mobile Communications Conference EPMCC´95*, Bologna, Italy, November 24-26, 1995, pp. 74-79
[117] B. E. Gschwendtner, F. M. Landstorfer, "3-D propagation modelling in microcells including terrain effects," *Proc. IEEE Intern. Personal, Indoor and Mobile Radio Conference PIMRC´95*, USA, 1995, pp. 532-536
[118] D. J. Cichon, W. Wiesbeck, "Comprehensive ray optical propagation models for indoor and outdoor environments: Theory and applications," *Proc. COMMSPHERE´95*, Eilat, Israel, January 22-27, 1995, pp. 201-208
[119] D. J. Cichon, T. C. Becker, M. Döttling, "Ray optical prediction of outdoor and indoor coverage in urban macro- and micro-cells," *Proc. IEEE Vehicular Technology Conference VTC'96*, Atlanta, USA, April 18-May 1, 1996, pp. 41-45
[120] J. Jakobsen, "Radio Propagation Measurements in Two Office Buildings," *COST-231 TD(90)28,* Copenhagen, Denmark, May 1990
[121] I. T. Johnson, W. Johnston, F. J. Kelly, "CW and Digital Propagation Behaviour from Outdoor Public Cells Measured in Customer Premises Cells," *COST-231 TD(90)82*, Paris, France, October 1990
[122] T. A. Wilkinson, "A Review of Radio Propagation into and Within Buildings," *COST-231 TD (90) 85*, Paris, France, October 1990
[123] "Propagation Models" subgroup, "Building penetration losses," *COST-231 TD(90)116 Rev.1,* Florence, Italy, January 1991
[124] A. M. D. Turkmani, J. D. Parsons, A. F. de Toledo, "Radio Propagation into Buildings at 1.8 GHz," *COST-231 TD(90)117,* Darmstadt, Germany, December 1990
[125] P. Backman, S. Lidbrink, T. Ljunggren, "Building penetration loss measurements at 1.7 GHz in micro cellular environments," *COST 231 TD(90)121*, Darmstadt, Germany, December 1990
[126] M. Sandén, "Building penetration loss measurements in the small cell environment," *COST-231 TD(90)122,* Darmstadt, Germany, December 1990

[127] E. Zollinger, "Dielectric Properties of Building Materials and Biological Tissues: A short Bibliographic Overview," *COST 231 TD(91)4*, Florence, Italy, January 1991
[128] CSELT, "Microcellular propagation: Measurements with low Base Station Antennas," *COST 231 TD(91)82*, Leidschendam, Netherlands, Sep. 1991
[129] J.-E. Berg, "Building Penetration Loss at 1700 MHz Along Line of Sight Street Microcells," *3rd PIMRC´92*, Boston, USA, October 1992, pp. 86-87
[130] J. Jimenez Delgado & J. Gavilan, "Indoors Penetration Results," *COST-231 TD(93)118*, Barcelona, Spain, Jan. 1993
[131] R. Gahleitner, "Wave Propagation into Urban Buildings at 900 and 1800 MHz," *COST-231 TD(93)92*, Grimstad, Norway, May 1993
[132] R. Gahleitner, "Radio Wave Propagation In and Into Urban Buildings," Ph.D. Thesis, Technical University of Vienna, 1994
[133] J.-E. Berg, "Comments on methods to assess penetration losses to be used in microcell models," *COST-231 TD(95)108*, Poznan, Poland, Sepember 1995
[134] J.-E. Berg, "Angle-dependent building penetration loss along LOS street microcells," *COST-231 TD(96)6*, Belfort, France, January 1996
[135] J. M. Keenan, A. J. Motley, "Radio coverage in buildings," *British Telecom Technology Journal*, vol. 8, no. 1, Jan. 1990, pp. 19-24
[136] J. Lähteenmäki, "Radiowave propagation in office buildings and underground halls," *Proc. of European Microwave Conference*, Espoo 1992, pp. 377-382
[137] P. Bartolomé, "Indoor propagation models validation," *COST 231 TD(93)51*, Barcelona, 1993
[138] S. Ruiz-Boqué, M Ballart, C. Clúa, R Agusti, "Propagation models for indoor mobile communications," *COST 231 TD(91)14*, Florence, Italy, 1991
[139] C. Törnevik, J.-E. Berg, F Lotse, "900 MHz propagation measurements and path loss models for different indoor environments," *Proc. IEEE VTC´93*, New Jersey, USA, 1993
[140] P. Karlsson, "Indoor radio propagation for personal communications services," Ph.D. Thesis, University of Lund, 1995
[141] J. Lähteenmäki, "Indoor propagation between floors at 855 MHz and 1.8 GHz," *COST 231 TD(94)37*, Lisbon, Portugal, 1994
[142] S. Ruiz-Boque, R. Agusti, J. Perez, "Indoor wideband channel characterization (900 and 1800 MHz) by means of a network analyzer," *COST 231 TD(91)71*, Barcelona, Spain, 1991
[143] S. Ruiz-Boqué, R Agusti, "Polarization diversity for indoor mobile communications," *COST 231 TD(93)7*, Barcelona, Spain, 1993
[144] H. Hashemi, "A study of temporal and spatial variations of the indoor radio propagation channel," *Proc. PIMRC´94*, pp. 127-134, 1994
[145] P. Karlsson, H. Börjeson, T. Maseng, "A statistical multipath propagation model confirmed by measurements and simulations in indoor environments at 1800 MHz," *Proc. PIMRC´94*, pp. 486-490, 1994
[146] R. P. Bultitude, "Measurement, characterization and modeling of indoor 800/900 MHz radio channels for digital communications," *IEEE Communications Mag.*, vol. 25, no. 6, pp. 5-12, June 1987

[147] D. Molkdar, "Review on radio propagation into and within buildings," *IEE Proc.-H*, vol. 138, no. 1, pp. 61-73, February 1991

[148] D. Cox, "Antenna diversity performance in mitgating the effects of portable radiotelephone orientation and multipath propagation," *IEEE Trans. on Comm.*, vol. 31, no. 5, pp. 620-628, 1983

[149] B. Fleury, D. Dahlhaus, "Investigations on the time variations of the wide-band radio channel for random receiver movements," *Proc. IEEE Int. Symp. on Spread Spectrum Techniques and Applications ISSSTA´94*, vol. 2, pp. 631-636, Oulu, Finland, 1994

[150] T. Huschka, "Ray-tracing models for indoor environments and their computational complexity," *Proc. PIMRC´94*, pp. 486-490, 1994

[151] W. Honcharenko, H. L. Bertoni, J. L. Dailing, J. Qian, H. D. Yee, "Mechanisms governing UHF propagation on single floors in modern office buildings," *IEEE Trans. on Vehicular Technology*, vol. 41, no. 4, pp. 496-504, 1992

[152] K. R. Schaubach, N. J. Davis, T. S. Rappaport, "A ray tracing method for predicting path loss and delay spread in microcellular environments," *Proc. IEEE VTC´92*, pp. 932-935, Denver, 1992

[153] P. Kreuzgruber, P. Unterberger, R. Gahleitner, "A ray splitting model for indoor radio propagation associated with complex geometries," *Proc. IEEE VTC´93*, NJ, USA, 1993, pp. 227-230

[154] D. J. Cichon, T. Zwick, J. Lähteenmäki, "Ray optical indoor modeling in multi-floored buildings: Simulations and measurements," *Proc. IEEE Intern. Antennas and Propagation Symposium AP-S'95*, Newport Beach, USA, 1995, pp. 522-525

[155] J. Lähteenmäki, "Testing and verification of indoor propagation models," *COST 231 TD(94)111*, Darmstadt, Germany, 1994

[156] M. Lebherz, W. Wiesbeck, (in German) "Beurteilung des Reflexions- und Schirmungsverhaltens von Baustoffen," ("Estimation of reflectivity and electromagnetic shielding properties of building materials"), *Bauphysik*, no. 12, 1990

[157] J. B. Hasted, M. A. Shah, "Microwave absorption by water in building materials," *Brit. Journal of Applied Physics*, vol. 15, 1964, pp. 825-835

[158] E. Zollinger, "Eigenschaften von Funkübertragungsstrecken in Gebäuden," ("Properties of indoor radio transmission"), Ph.D. Thesis, no. 10064, Swiss Federal Institute of Technology Zürich (ETH), Zürich, Nov. 1993, pp. 20-28

[159] T. Klemenschits, "Mobile Communications in Tunnels," Ph.D. Thesis, Technical University of Vienna, Austria, 1993

[160] K. Gunmar, "Broadband technique for car to car communication at 60 GHz," *COST-231 TD(91)41*, Lund, Sweden, 1991

[161] Z. Ghebretensae, "Simulations of beacon-vehicle communications for DRIVE applications," *COST-231 TD(92)53*, Leeds, United Kingdom, 1992

[162] K. Gunmar, "Simulation of the GSM-SDCCH-channel for LOS microcell communication for DRIVE applications," *COST-231 TD(92)87*, Helsinki, Finland, 1992

[163] J. Wickman, "Measurements and simulations of wave propagation in a corridor at 1800 MHz," *COST 231 TD(90)124*, Darmstadt, Germany, 1990

[164] T. Klemenschits, A. L. Scholtz, E. Bonek, "Microwave Measurements in Scaled Road Tunnels Modelling 900 MHz Propagation," *Proc. 43rd IEEE Vehicular Technology Conf.*, May 1993, Secaucus, NJ, USA, pp. 70 - 72

[165] T. Klemenschits, E. Bonek, "Radio Coverage of Road Tunnels at 900 and 1800 MHz by Discrete Antennas," *Proc. of the 5th Intern. Symposium on Personal, Indoor and Mobile Radio Communications*, 411 - 415, The Hague, The Netherlands , 1994

[166] T. Klemenschits, "Wave propagation in road tunnels - The method of image antennas," *COST-231 TD(91)33*, Lund, Sweden, 1991

[167] CSELT-SIRTI (Italy), "Propagation measurements inside tunnels," *COST-231 TD(91)83*, Leidschendam, 1991

[168] DRIVE Consortium V2014-ICAR, "System and radiating elements analysis for the transmission of the GSM signals in tunnels," *COST-231 TD(93)59*, Grimstad, Norway, 1993

[169] M. Göller, K. D. Masur, (in German) "Ergebnisse von Funkkanalmessungen im 900-MHz-Bereich auf Neubaustrecken der Deutschen Bundesbahn," ("Results of radio channel measurements at 900 MHz along German high-speed railway lines"), Teil 1 u. 2, Nachrichtentechnik Elektronik 42, pp. 143 ff, 1992

[170] R. Gahleitner, T. Klemenschits, R. Stepanek, "First results of a direct-conversion chanel sounder (DCCS-1800) recorded in a road tunnel," *COST-231 TD(93)88*, Grimstad, Norway, 1993

[171] M. Uhlirz, "Concept of a GSM-based Communication System for High-Speed Trains," *Proc. IEEE VTC´94*, Stockholm, Sweden, pp. 1130 - 1134

[172] M. Uhlirz, "Adapting GSM for Use in High-Speed Railway Networks," Ph.D. Thesis, Technical University of Vienna, Austria, 1995

[173] R. H. Rækken, M. Sneltvedt, "Using an autonomous measurement system to evaluate GSM coverage along railways", in Proc. Nordic Radio Symposium 1995 (NRS'96), Saltsjöbaden, Sweden, April 1995, pp. 201-206

[174] G.G. Cook, A.P. Anderson, A.S. Turnbull, "Spectral Incremental Propagation (SIP) procedure for fast calculation of scattered fields from conducting bodies", IEE Proc., Vol. 136, Pt. H, No.1, Feb. 1989, pp. 34-38